



# Detoxification of tetracycline and synthetic dyes by a newly characterized *Lentinula edodes* laccase, and safety assessment using proteomic analysis

Shuxue Zhao<sup>c,1</sup>, Xiaohang Li<sup>c</sup>, Xingdong Yao<sup>a</sup>, Xuyang Liu<sup>a</sup>, Chao Pan<sup>c</sup>, Lizhong Guo<sup>a</sup>, Jie Bai<sup>c</sup>, Tiantian Chen<sup>c</sup>, Hao Yu<sup>a,\*</sup>, Chunhui Hu<sup>b,\*</sup>

<sup>a</sup> Shandong Provincial Key Laboratory of Applied Mycology, School of Life Sciences, Qingdao Agricultural University, Qingdao, Shandong Province 266109, China

<sup>b</sup> Instrumental Analysis Center of Qingdao Agricultural University, Qingdao, Shandong Province 266109, China

<sup>c</sup> College of Environmental Science and Engineering, Ocean University of China, Qingdao, Shandong Province 266100, China

## ARTICLE INFO

Edited by Professor Bing Yan

### Keywords:

Fungal laccase  
Proteomic, biodegradation  
Tetracycline  
Dyes, safety assessment

## ABSTRACT

Fungal laccase has strong ability in detoxification of many environmental contaminants. A putative laccase gene, *LeLac12*, from *Lentinula edodes* was screened by secretome approach. *LeLac12* was heterogeneously expressed and purified to characterize its enzymatic properties to evaluate its potential use in bioremediation. This study showed that the extracellular fungal laccase from *L. edodes* could effectively degrade tetracycline (TET) and the synthetic dye Acid Green 25 (AG). The growth inhibition of *Escherichia coli* and *Bacillus subtilis* by TET revealed that the antimicrobial activity was significantly reduced after treatment with the laccase-HBT system. 16 transformation products of TET were identified by UPLC-MS-TOF during the laccase-HBT oxidation process. Gas chromatography-mass spectrometry (GC-MS) analysis revealed that *LeLac12* could completely mineralize ring-cleavage products. *LeLac12* completely catalyzed 50 mg/L TET within 4 h by adding AG (200 mg/L), while the degradation of AG was above 96% even in the co-contamination system. Proteomic analysis revealed that central carbon metabolism, energy metabolism, and DNA replication/repair were affected by TET treatment and the latter system could contribute to the formation of multidrug-resistant strains. The results demonstrate that *LeLac12* is an efficient and environmentally method for the removal of antibiotics and dyes in the complex polluted wastewater.

## 1. Introduction

The excessive use and discharge of antibiotics and dyes in water and soil are increasing annually, severely threatening the ecosystem and human health (Bhardwaj et al., 2022). Over hundreds and thousands of tons of antibiotics and 7 million tons of dyes are used every year worldwide (Bhagat et al., 2020; Gui et al., 2019). Antibiotics are widely used in agricultural, commercial, and pharmaceutical fields for treating microbial infections and protecting the health of humans and animals. As one group of the broad-spectrum antibiotics, tetracycline (TET) is the second most widely used in human medicine and aquaculture, and has been detected in wastewater and natural water systems (Zuo et al., 2022). TET has a stable structure of four aromatic rings, which is difficult to be degrade and absorbed. The harms of TET to the ecosystem are mainly reflected in the development of antibiotic-resistance. Acid green 25 (AG) is an organic sulfonic acid dye, which can cause eye and skin

irritation and is toxic to aquatic organisms (Jain et al., 2018). The treatment of antibiotics and dyes in the environment is increasingly becoming a critical problem.

Fungi have a strong ability to metabolize antibiotics by producing extracellular ligninolytic enzymes such as laccase (Solanki et al., 2013; Lark et al., 2019; Adak et al., 2016). Laccase, a multi-copper oxidase, is widely distributed in bacteria, fungi and plants (Khan et al., 2014). Due to its low substrate specificity and high catalytic activity, laccase has been applied in environmental remediation, paper industry, and biofuel production (Kishor et al., 2021; Singh et al., 2016). Recent studies have shown that laccase can effectively degrade tetracycline (Suda et al., 2012; Weng et al., 2012), oxytetracycline (Tian et al., 2020; Sun et al., 2017) and dyes (Jeon et al., 2017; Adak et al., 2016; Songulashvili et al., 2006). To date, there have been no reports on the application of laccase from *Lentinula edodes* for the degradation of TET and dyes.

As the largest productive edible mushroom in the world, *L. Edodes*,

\* Correspondence to: 700 Changcheng Road, Chengyang District, Qingdao, Shandong Province, China

E-mail addresses: [yuhaosunshine@163.com](mailto:yuhaosunshine@163.com) (H. Yu), [hollyhuchunhui@163.com](mailto:hollyhuchunhui@163.com) (C. Hu).

<sup>1</sup> First author:

<https://doi.org/10.1016/j.ecoenv.2024.116324>

Received 6 February 2024; Received in revised form 9 April 2024; Accepted 11 April 2024

Available online 17 April 2024

0147-6513/© 2024 The Authors. Published by Elsevier Inc. This is an open access article under the CC BY license (<http://creativecommons.org/licenses/by/4.0/>).

can secrete plenty of lignocellulolytic enzymes capable of degrading lignin and cellulose. And these enzymes could be applied in bioremediation. It has been reported that the genome of *L. edodes* contains several laccase genes (Chen et al., 2016). The laccase of *L. edodes* had a great contribution to the degradation of lignocellulose and they were also used for other purposes (Liu et al., 2020; Tsujiyama et al., 2013; Wong et al., 2012). However, only a small portion of the predicted laccase functions have been experimentally characterized. Laccase produces corresponding intermediate metabolites during the degradation of pollutants, which is of great importance for the assessment of their biological toxicity. The biological toxicity of the biodegraded products of antibiotics and dyes has been evaluated by microbial growth inhibition or antibacterial activity tests, and by plant seed germination tests (Blázquez, et al., 2018; García-Delgado et al., 2018; Iark et al., 2019).

With the development of omics technology, proteome has become an important tool to identify and quantify proteins in different biological samples as well as secreted proteins (Yang et al., 2021; Zhao et al., 2021). In many studies, proteomics methods have been used to obtain the expression profiles of intracellular and extracellular enzymes produced by white-rot fungus (WRF) and to identify proteins, peptides, and their post-translational modifications (Mahajan et al., 2010; Hori et al., 2014). In addition, high-throughput proteomic analysis can be used to identify changes in protein abundance due to microbial utilization of different substrates or adaptive responses in different environments (Li et al., 2012; Hartmann et al., 2014; Chen et al., 2018).

The *L. edodes* LE-W1, as a commercial production strain, produces high amounts of laccase and has a strong ability to degrade TET and decolorize dyes. In this study, the secreted proteins of *L. edodes* LE-W1 during the mycelium growth period were analyzed using proteomic techniques. An extracellular fungal laccase named LeLac12 was identified and heterologously expressed. The degradation rate of TET and AG in combination with mediators was investigated. And the degradation of TET was enhanced by adding AG. The toxicity of their metabolites was investigated by microbial growth inhibition assays and proteomics. The objectives of this study were (1) to provide an efficient method to identify fungal laccases that can be used to degrade environmental pollutants, and (2) to discover a novel fungal laccase from *L. edodes* LE-W1 that has great potential for the bioremediation of environmental pollutants in complex polluted wastewater, (3) to evaluate the toxicity of TET, AG and their metabolites to *Escherichia coli* via proteomics and to prove that the fungal laccase LeLac12 can convert TET and AG into non-toxic products.

## 2. Material and methods

### 2.1. Strains and chemicals

The strain *L. edodes* LE-W1 used in this study was provided by the Laboratory of Mushroom Precision Breeding (mushroomlab.cn). The competent cells of *E. coli* DH5 $\alpha$  and *Pichia pastoris* GS115 were purchased from TransGen Biotech Co., Ltd (Beijing, China). The strain *L. edodes* LE-W1 was cultured and transferred in potato dextrose agar (PDA medium: extract from 200 g/L potato, 20 g/L dextrose, 20 g/L agar) in darkness at 25 °C. At the vegetative growth stage, *L. edodes* can secrete a variety of proteins by utilizing the substrate for mycelial growth, and explore the types of secreted proteins.

PDA medium, glucose, 1-hydroxybenzotriazole (HBT), and 2,2'-azino-bis (3-ethylbenzothiazoline-6-sulfonate) (ABTS) were purchased from Sangon Co., Ltd. (Shanghai, China). Yeast nitrogen base without amino acids (YNB), geneticin (G418), peptone, yeast extract, and TET (CAS: No. 64-75-5, AR) were purchased from Beijing Solarbo Technology Co., Ltd. Trifluoroacetic acid (TFA) and acetonitrile of mass grade were purchased from Aladdin Ltd (Shanghai, China). All other reagents used in this study were of analytical grade if not described specifically.

### 2.2. Secretome analysis

The mycelia of strain *L. edodes* LE-W1 were cultivated on sawdust medium (mixing sawdust and rice bran at a ratio of 4:1 (w/w)) to a water content of ~65% and a weight of 2.0 kg in polyethylene bags. The sawdust medium was cultivated at 22 °C until the mycelia had occupied the entire medium. 20 g of sawdust medium with mycelia was added to 80 mL of PBS buffer (pH 8.0) and shaken at 25 °C, 125 rpm for 30 min. The mixture was centrifuged at 6000 g for 30 min, and the supernatant was then transferred to a new centrifugation tube. Trichloroacetic acid (TCA) was added to the supernatant to a final concentration of 10% (w/v) and the secreted proteins were precipitated at -20 °C overnight (Cai et al., 2017). The protein concentration was measured by the Bradford method (Song et al., 2018). The peptide was prepared using the Filter Aided Sample Preparation (FASP) method (Wiśniewski et al., 2009; Zhao et al., 2022). 100  $\mu$ g of the protein sample was added to 300  $\mu$ L of UA buffer (8 M urea, 100 mM Tris-HCl, pH 8.0), and then diluted into the FASP ultrafiltration tube, centrifuged at 10,000  $\times$  g for 30 min. The protein was washed once with 300  $\mu$ L UA buffer. 100  $\mu$ L UA buffer containing 50 mM iodoacetamide (IAA) was added to the centrifuge tube and incubated for 30 min in darkness. The protein sample was washed by 200  $\mu$ L UA buffer thrice and 300  $\mu$ L 50 mM ammonium bicarbonate (ABC) twice. Peptide digestion was performed by adding 2  $\mu$ g of trypsin (dissolved in 50 mM ABC) to the ultracentrifugation tube, and incubated at 37 °C for 12 h. The reaction was terminated by adding TFA to the final concentration of 0.4%. The peptide concentration was measured using NanoDrop One (Thermo Fisher) at 280 nm. The peptide samples were evaporated, and stored at -80 °C for further analysis.

LC-MS/MS analysis was performed by an EASY-Nano coupled with Orbitrap Fusion™ Tribrid™ detectors (Thermo Fisher). Raw data were normalized by Proteome Discovery 3.0. The treated data were further analyzed by Perseus software (Tyanova et al., 2016).

### 2.3. Protein expression and purification

The strain *L. edodes* LE-W1 was inoculated into the PDA plate, and then cultivated in the dark at 25 °C for 7 days. The mycelia were scratched from the cellophane and ground with liquid nitrogen. Total RNA was extracted using the Trizol method according to the instructions (Takara, Japan). Reverse transcription was performed using the Hifair III 1st Strand cDNA Synthesis Kit (Yeasen Biotechnology (Shanghai) Co., Ltd.). The gene was amplified by primers in [supplementary material \(Table S1\)](#) and then ligated to the pPIC9k plasmid. The recombinant plasmid was electroporated into *P. pastoris* GS115 to express the protein. The protein was loaded onto a Ni-NTA (GE, 316 USA) column and purified according to Yu et al. (2017) reported. The purified LeLac12 was detected by SDS-PAGE. The construction of the recombinant strain and the expression of LeLac12 were described in the [supplementary material](#).

### 2.4. Characterization and kinetic analysis of recombinant LeLac12

Laccase activity was measured at room temperature using ABTS as substrate (Sun et al., 2013). The oxidation of ABTS was measured at 420 nm in 0.05 M sodium-acetate buffer (pH 4.5). One unit of laccase activity was defined as the amount of enzyme required to oxidize 1  $\mu$ M ABTS per minute under assay conditions.

To find the best mediator, ABTS, 3-aminobenzoic acid (3ABA), 2,6-dimethoxyphenol (DMP), o-tolidine (TOD), guaiacol (GUA) and levodopa (L-dopa) were used as mediators for the laccase activity assay, the specific measurement wavelength and molar extinction coefficient of each substrate are listed in [Table S2 \(Lee et al., 2012\)](#).

The effect of pH (1.0–8.0) on LeLac12 activity was measured in 50 mM malonate buffer and the effect of temperature (20–90 °C) was measured at 50 mM malonate buffer (pH 3.0). The thermal stability of LeLac12 was determined at 60 °C for 0.5, 1.0, 1.5, 2.0, and 4.0 h,

respectively. The enzyme activity of LeLac12 was determined by adding different metal ions ( $\text{Ca}^{2+}$ ,  $\text{Cd}^{2+}$ ,  $\text{Cu}^{2+}$ ,  $\text{Co}^{2+}$ ,  $\text{Li}^+$ ,  $\text{Mg}^{2+}$ ,  $\text{Mn}^{2+}$ ,  $\text{Mo}^{6+}$ ,  $\text{Na}^+$ ,  $\text{K}^+$ , and  $\text{Zn}^{2+}$ ) at a final concentration of 5 mM and 10 mM. The effect of various inhibitors, such as EDTA, methanol, acetonitrile, acetone, and ethanol on LeLac12 activity was assayed.

### 2.5. Homology modeling, structural prediction and molecular docking

The 3D homology model of LeLac12 was generated via the Swiss Model online server (<https://swissmodel.expasy.org/>) (Biasini et al., 2014). *Trametes hirsuta* laccase (PDB:3pxl.1.A) (type-II Cu-depleted fungal laccase) was used as a reference protein model. The structural analysis of LeLac12 was performed using InterPro (<http://www.ebi.ac.uk/interpro/search/sequence/>). The phylogenetic tree was constructed using MEGA X software based on the amino acids of LeLac12, published laccase sequences, and 14 laccase sequences from *L. edodes* reported by Yan et al. (2019). Motif prediction and amino acid abundance in the motif were performed on the MEME website (<https://meme-suite.org/meme/tools/meme>).

AutoDock Vina was selected as the molecular docking program. The structures of the small molecules TET and AG were retrieved from the PubChem database. LeLac12 was docked with the compounds TET and AG, respectively. Two compounds were designated as ligands and proteins as receptors. PyMOL (version 4.3.0) software (<https://pymol.org/>) was used to separate the original ligand and protein structure, dehydrate, and remove organic material. AutodockTools (<http://mglttools.scripps.edu/downloads>) was used for hydrogenation, checking the charge, determining the atom type as AD4 type, calculating the gasteiger, and constructing a docking grid box for the protein structure, selecting the reversible bonds of the ligand. After using Vina docking, the score for the combination of protein with the small molecules TET and AG was calculated, Three-dimensional and two-dimensional force analysis and visualization was performed using Discovery Studio software.

### 2.6. Degradation and detoxification of TET by LeLac12

The enzymatic degradation of TET was evaluated in different mediators using a 50 mM malonate buffer (pH 3.0). The reaction mixture contained (final concentration): 50 mg/mL TET, 0.25 mM HBT or ABTS or no mediator, 50 mM malonate buffer (pH 3.0) and 1 U/mL purified LeLac12. The degradation was carried out at 30 °C for 4 h. Two volumes of methanol were added to terminate the reaction. The concentration of TET was measured with the Waters 2695 HPLC system (Waters, USA) equipped with a DAD detector using a Waters-Spherisorb ODS2-C18 column (Waters, 4.6 mm × 250 mm, 5 μm) at 30 °C. Isocratic elution (30% acetonitrile and 70% 0.1% formic acid, v/v) was performed at a flow rate of 1.0 mL/min. The metabolites of the degradation of TET by LeLac12 were analyzed by ultra-high-performance liquid chromatography-high resolution mass spectrometry (HPLC-ESI-Q-TOF-MS, HPLC: ThermoFisher Ultimate 3000, MASS: Brooke maXis) with symmetry C18 column (2.1 × 150 mm, 5 μm, Waters). The positive ionization mode was used with 1 μL sample. Samples were analyzed with 0.1% formic acid in the mobile phase from 10% to 100% methanol within 30 min at a flow rate of 0.2 mL/min. The temperature and flow rate of the drying gas, and the capillary voltage were set as 180 °C, 6 L/min, and 4.5 KV. Mass spectral data were analyzed by MSDIAL v4.70.

Growth inhibition assays were performed with *E. coli* and *B. subtilis* as previously described by Tian et al. (2020) with minor modifications. The LeLac12 degradation products of TET were heated and filtered through a 0.22 μm filter membrane. The degradation mixture was mixed with the same volume of Luria-Bertani broth (LB). 1% (v/v) *E. coli* and *B. subtilis* strains were incubated in the LB medium, respectively. The same system with intact TET and without TET was used as control. After culturing for 10 h at 37 °C, OD<sub>600 nm</sub> was determined to evaluate the antibacterial activity of TET degradation products.

### 2.7. Degradation and decolorize of AG by LeLac12

Purified LeLac12 was used to decolorize three types of synthetic dyes. These were reactive yellow (RY, azo dye), methyl orange (MO, azo dye), Coomassie brilliant blue G250 (CG-250, triphenylmethane dye), crystal violet (CV, triphenylmethane dye), Bromophenol blue (BB, triphenylmethane dye), active blue KNR (AB-KNR, anthraquinone dye), acid green 25 (AG, anthraquinone dye) and acid blue 40 (AB-40, anthraquinone dye). The chemical structures and maximum absorption values of these dyes are listed in Table S3. The decolorization mixture in a total volume of 1 mL contained (final concentration): 50 mM malonate buffer (pH 3.0), 100 mg/L dyes, and purified LeLac12 (50 U/L). The degradation rate of the dyes was determined after 24 h. Decolorization was monitored by measuring the absorbance of the reaction mixture at 420 nm for RY and BB, 465 nm for MO, 584 nm for CG-250 and CV, 590 nm for AB-KNR and AB-40, and 612 nm for AG. The decolorization rate was calculated using the following formula: Decolorization rate (%) =  $(A_0 - A_t) / A_0 \times 100\%$ .  $A_0$  was the initial absorbance of the reaction and  $A_t$  was the absorbance of the reaction mixture at time  $t$ .

The enzymatic degradation of AG was tested in different mediators using a 50 mM malonate buffer (pH 3.0). The reaction mixture contained (final concentration): 200 mg/L AG, 0.25 mM HBT or ABTS or no mediator, 50 mM malonate buffer (pH 3.0) and 50 U/L purified LeLac12.

To identify the intermediates of degradation, 400 mg/L AG was transformed by 50 U/L purified LeLac12 for 4 h and the reaction was terminated by addition of HCl to pH 2.0. The degradation intermediates were extracted three times with equal volumes of ethyl acetate. The pooled ethyl acetate was mixed, dried with anhydrous sodium sulfate, and evaporated to dryness with nitrogen gas. The dried products were redissolved in 1 mL pyridine, derivatized with BATFA/TMCS (99:1) according to the methods described by Zhao et al. (2021) and analyzed by GC-MS (TSQ8000Evo, Thermo Fisher). The injection temperature was 250 °C, and a TG-5SILMS column (30 m × 0.25 mm i.d., 0.25 μm film thickness; J&W Scientific) was used. The column temperature was maintained at 50 °C for 2 min, then linearly increased from 50 °C to 300 °C at 5 °C/min and maintained at 300 °C for 2 min. Helium gas was used as the carrier gas at a flow rate of 1.0 mL/min. The mass selective detector was operated in electron ionization mode at 70 eV and a scan range  $m/z$  of 50–500.

### 2.8. Co-degradation of TET and AG by LeLac12

The purified LeLac12 was used to degrade TET and AG in the following mixtures (final concentration): 200 mg/L AG, 50 mg/L TET, 0.25 mM and 1 mM HBT or ABTS or without mediator, 50 mM malonate buffer (pH 3.0) and 1 U/mL purified LeLac12. All degradation reactions were carried out at 30 °C for 4 h. Samples were taken to determine the degradation of TET and AG.

### 2.9. Safety risk assessment

The safety of the TET, AG, and their degradation products were assessed according to the cellular response of *E. coli* cells. The *E. coli* were incubated at 37 °C, 180 rpm for 6 h with TET (named TET Group), TET degradation products (named TETDeg Group), AG (named AG Group), AG degradation products (named AGDeg Group), and sterile distilled water (named CK Group), respectively. The proteins were extracted and digested by STRap methods in supplementary material (Yu et al., 2023; Zougman et al., 2014). R packages were used to construct Venn diagrams, Principal component analysis, and volcano plots. The KEGG enrichment was performed using wkomics (<https://www.omicsoft.com/wkomics/main/>) analysis platform (Wang et al., 2018). Using TBtools software to perform GO enrichment analysis (Chen et al., 2023).

### 3. Results and discussion

#### 3.1. *L. edodes* LE-W1 secretome analysis and laccase identification

The growth of *L. edodes* can be divided into hyphal knot growth, light-induced brown film formation by the mycelia, primordium initiation, fruiting body development mycelium growth and fruiting body growth stage (Huang et al., 2020). During physiological node growth, the carbohydrate-active enzymes (CAZymes) play a major role in substrate degradation (Davies et al., 2016). The secreted proteins in vegetative growth of solid media cultivated *L. edodes* LE-W1 cultured on solid media were analyzed (Fig. 1a). A total of 935 proteins were detected (Dataset S1), of which most proteins (151) belong to the CAZymes protein family. 11, 3, and 4 proteins were detected in protease, esterase, and phosphatase, and 766 other proteins such as hypothesis protein and unknown function protein were detected (Fig. 1b). The number of other proteins and CAZymes accounted for 81.93% and 16.14% of the total proteins, respectively. The abundance of other proteins and CAZymes was 49.33% and 47.86%, respectively (Fig. 1c). CAZymes are divided into various enzyme classes and families thereof that catalyze the breakdown, biosynthesis, and modification of glycoconjugates, oligo- and polysaccharides, including the auxiliary activity (AA) family, the glycoside hydrolase (GH) family, the glycosyltransferase family (GT), polysaccharide lyase family (PL), carbohydrate esterase family (CE), and carbohydrate-binding module family (CBM) (Levasseur et al., 2013). The characterized AA1 enzymes are multicopper oxidases that use diphenols and related substances as donors and oxygen as an acceptor. A total of 151 CAZymes proteins in *L. edodes* LE-W1 were detected in secretory proteome, 96 in the GH family, 34 in the AA family, and 13, 4, 3, and 1 protein were detected in the CE, GT, PL, and CBM, respectively (Fig. 1d). The abundance of GH proteins and AA proteins accounted for 57.87% and 39.31% of the abundance of CAZymes proteins, respectively (Fig. 1e). The AA family is currently categorized into 3 subfamilies including laccases, ferroxidases, and laccase-like multicopper oxidases (Drula et al., 2022). 7 laccases were identified (Table S4). By comparing

the peak areas and their homology with AOX45445.1 and BAD98306.1 (Fig. S1), A0A1Q3E0A2 (named LeLac12) was selected for further investigation.

Using *Trametes hirsuta* laccase (PDB: 3pxl. 1) crystalline protein as a model and homologous modeling, three Cu ions were found in LeLac12. Within 4 Å, Cu4 was associated with 5 residues, interacted with 3 PLIPs, and has 3 interactions with the A-chain. The metal binding sites include A: H.127, A: H.424, and A: H.472. Within 4 Å, Cu5 was associated with 5 residues, namely H.80, H.82, W.123, H.125, and H.474 on the A-chain, and interacted with 3 PLIPs. Within 4 Å, Cu7 was associated with 4 residues, namely H.80, H.82, H.422, and H.424 on the A-chain, and interacted with 3 PLIPs (Fig. S2a). In the secondary structure of LeLac12, there were 9  $\alpha$ -spirals, 40 pieces  $\beta$ -folds, and 34 pieces  $\beta$ -corners. Most fungal laccases contain a total of 520–550 amino acids and a signal peptide sequence (about 20 residues) (Wang et al., 2017). LeLac12 had 523 amino acid residues, 8 N-glycosylated, and 17 signal peptide sequences. It was predicted that 38–488 belongs to Cu oxidase family, including Cu-oxidase\_N (29–146), Cu-oxidase\_2nd (159–311), Cu-oxidase\_C (373–491) domain (Paysan-Lafosse et al., 2022). The result shows that LeLac12 is a typical fungal laccase. LeLac12 has four conserved copper-binding motifs of typical fungal laccases: Cu I (HWHGFFQ), Cu II (HSHLSTQ), Cu III (HPFHLHG), and Cu IV (HCHIDWHL) (Giardina et al., 2010; Yang et al., 2014). Multiple alignments of the deduced amino acid sequence of LeLac12 with other laccases based on MEGA X (Fig. S2b). LeLac12 had 31.39% and 22.79% identity with *Aspergillus niger* ATCC 1015 (EHA27936) and *B. subtilis* (P07788), respectively. It was 47.89%, 50.91%, and 59.69% identical to *Volvariella volvacea* (AAO72981), *Pleurotus* sp. (Q12729), and *Lentinus sajor caju* (AAG27433), respectively (Fig. S2c). AAO72981 and Q12729 were selected to compare the amino acid sequences with LeLac12. Four motifs were found, and the amino acid abundance of each domain was different. However, the amino acids in the three laccases were conservative (Fig. S2d).

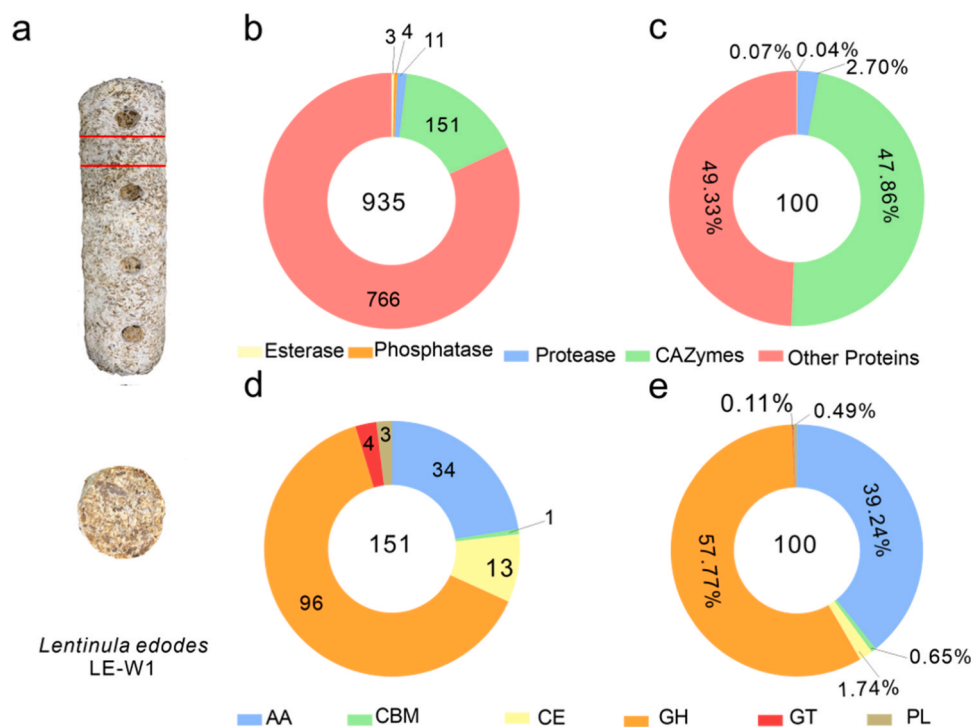


**Fig. 1.** Protein sample acquisition and secretome analysis of *L. edodes* LE-W1. a, Mycelium growth of *L. edodes* LE-W1 during the stage of sample acquisition; b, The classification and quantity of *L. edodes* LE-W1 proteins; c, The classification and relative abundance of *L. edodes* LE-W1 proteins; d, The classification and quantity of *L. edodes* LE-W1 CAZymes; e, The classification and relative abundance of *L. edodes* LE-W1 CAZymes.

### 3.2. Purification and properties of LeLac12

Wong et al. (2012) heterologously expressed Lcc1A and Lcc1B in *P. pastoris*, and Liu et al. (2020) successfully expressed *L. edodes* laccase LeLac using *P. pastoris* as a host cell. *P. pastoris* was selected as the host cell for heterologous expression of LeLac12. Under denaturing conditions, the molecular size of LeLac12 was detected by gel electrophoresis at approximately 110 kDa. A zymogram reaction of LeLac12 was performed with ABTS, and the size of the protein was found to be the same as that of SDS-PAGE (Fig. 2a). Compared with pPIC9k-GS115, a protein of about 110 kDa could be expressed from the recombinant strain GS115-pPIC9k-LeLac12, which could be oxidized with ABTS, but the size of the obtained protein was different from the predicted size of LeLac12 (57.25 kDa), which was probably due to the formation of a protein dimer (Thurston, 1994).

The purified LeLac12 was then subjected to kinetic analysis. LeLac12 had the highest affinity for ABTS (Fig. 2b), followed by DMP. It had a low affinity for GUA and TOD, but no significant affinity for 3ABA and L-dopa. When ABTS was used as a substrate, LeLac12 had the highest activity at pH 3.0. When the pH value was higher than 6.0, all oxidizing activity was lost (Fig. 2c). This indicates that LeLac12 was active in the acidic range. LeLac12 shows maximum activity at 30 °C (Fig. 2d). At 60 °C, 71.0% of the activity was still preserved. When the incubation temperature reached 90 °C, the activity of LeLac12 was only 4.93%. The temperature stability of LeLac12 protein was measured at 60 °C for 4 h, and the activity of LeLac12 decreased with the extension of storage time. Approximately 68% of the original enzyme activity remained after 4 h at 60 °C (Fig. 2e). LeLac lost 52% of the enzyme activity when stored at 60 °C for 10 min (Liu et al., 2020), while LeLac12 exhibited higher temperature stability. Different sulfate or chloride salts had different effects on the activity of LeLac12. When the final concentration was 5 mM/10 mM,  $\text{Cu}^{2+}$ ,  $\text{Mg}^{2+}$ ,  $\text{Zn}^{2+}$ , and  $\text{Cd}^{2+}$  could promote the activity of LeLac12 (Fig. 2f). The promoting effect of 10 mM  $\text{Cu}^{2+}$  on LeLac12 was 215.58%, and other sulfates and chlorine salts inhibited LeLac12. It was suggested that  $\text{Co}^{2+}$  is the key to inactivate LeLac12 activity. With increasing EDTA concentration, the inhibition rate of LeLac12 activity increased, suggesting that LeLac12 is a metal-dependent enzyme. Organic solvents (methyl alcohol, ethyl alcohol, acetonitrile and acetone) significantly inhibited LeLac12 activity (Table S5).

After incubation at pH 3.0 and 30 °C, the enzyme reaction follows Michaelis-Menten kinetics. The apparent  $K_m$  and  $k_{cat}$  of ABTS in 50 mM malonic acid buffer were 10.36  $\mu\text{M}$  and 31.77  $\text{s}^{-1}$ , respectively, and the  $k_{cat}/K_m$  value was 3060  $\text{s}^{-1} \text{mM}^{-1}$  (Fig. 2g). The apparent  $K_m$  and  $k_{cat}$  value of DMP in 50 mM malonic acid buffer were 37.38  $\mu\text{M}$  and 318.87  $\text{s}^{-1}$ , respectively, and the  $k_{cat}/K_m$  value was 8530  $\text{s}^{-1} \text{mM}^{-1}$  (Fig. 2h). By kinetic analysis, LeLac12 showed a higher affinity to ABTS than to DMP, which is consistent with other fungal laccases (Liu et al., 2020; Wong et al., 2012).

### 3.3. Molecular docking of LeLac12 with TET and AG

Molecular docking has been proved to be a valid tool for substrate selection based on previous studies (Xu et al., 2022). Exploring the interaction mechanism between laccase and substrate by molecular docking. The binding energy between TET and protein was  $-7.6 \text{ kcal/mol}$ , and the binding energy of laccase and TET reported by Han et al. (2023) was  $-7.7 \text{ kcal/mol}$ . The results indicated that the interaction between the ligand TET and the receptor laccase was spontaneous (Fig. 3a). There was a clear relationship between the dye molecule and the active site of the protein. The binding mechanism can range from conformational selection models to induced coordination models (Mitra et al., 2023).

The binding energy between LeLac12 and dyes can be found in Table S6. The results show that the binding energy of anthraquinone dyes was lower than that of the other two types of dyes, indicating that LeLac12 can degrade anthraquinone dyes more efficiently. The binding energy between AG and LeLac12 was  $-8.6 \text{ kcal/mol}$ . The combination form was shown in Fig. 3b, and the lowest energies for GILCC1 were  $-6.61 \text{ kcal/mol}$  and  $-6.28 \text{ kcal/mol}$  for Crystal Violet and Malachite Green, respectively (Morales-Álvarez et al., 2018). The results showed that the interaction between AG and the receptor laccase was spontaneous. Compared to AG, the molecular docking results of TET showed that the protein could degrade AG more easily, which is consistent with the experimental results.

### 3.4. Transformation and detoxification of TET by LeLac12

According to the HPLC results, TET was detected at 0 h ( $R_t=4.0 \text{ min}$ )

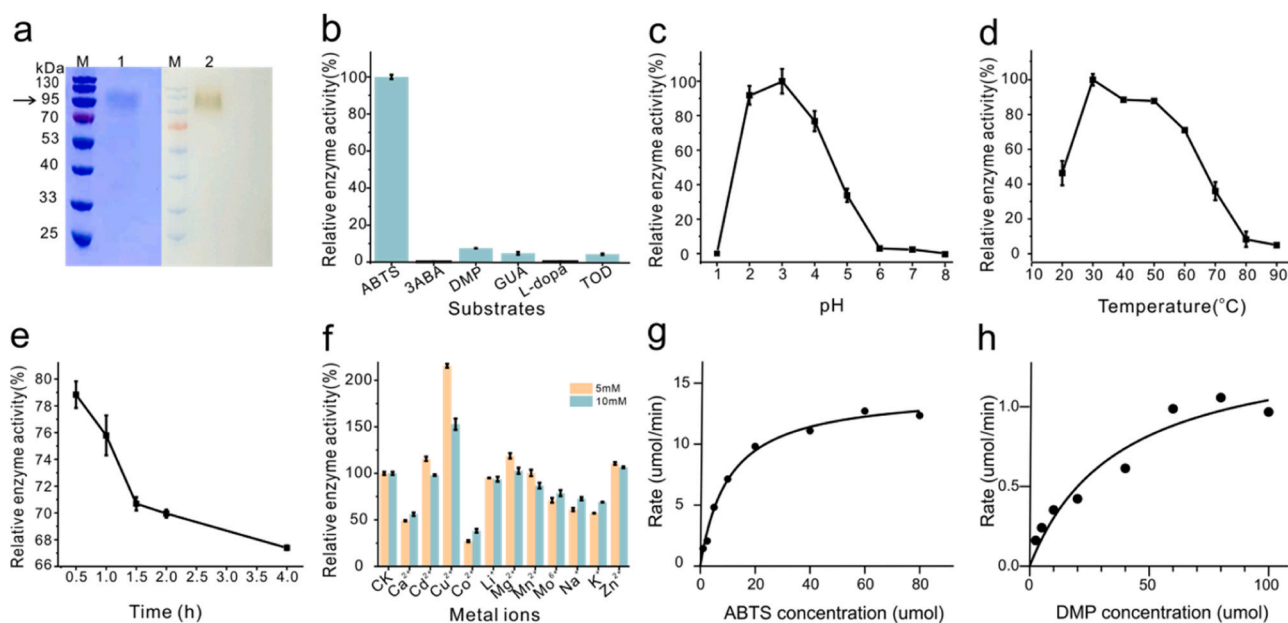


**Fig. 2.** Analysis catalytic characteristic of LeLac12. a, SDS-PAGE and zymogram of purified LeLac12. M: RealBand protein marker, 1: denatured LeLac12; 2: LeLac12; b, Substrate specificity of LeLac12; c, Effect of pH on enzyme activity of LeLac12; d, Effect of temperature on enzyme activity of LeLac12; e, Temperature stability of LeLac12; f, Effect of metal ions on the activity of the LeLac12; g, Kinetic studies of ABTS for LeLac12; h, Kinetic studies of DMP for LeLac12.

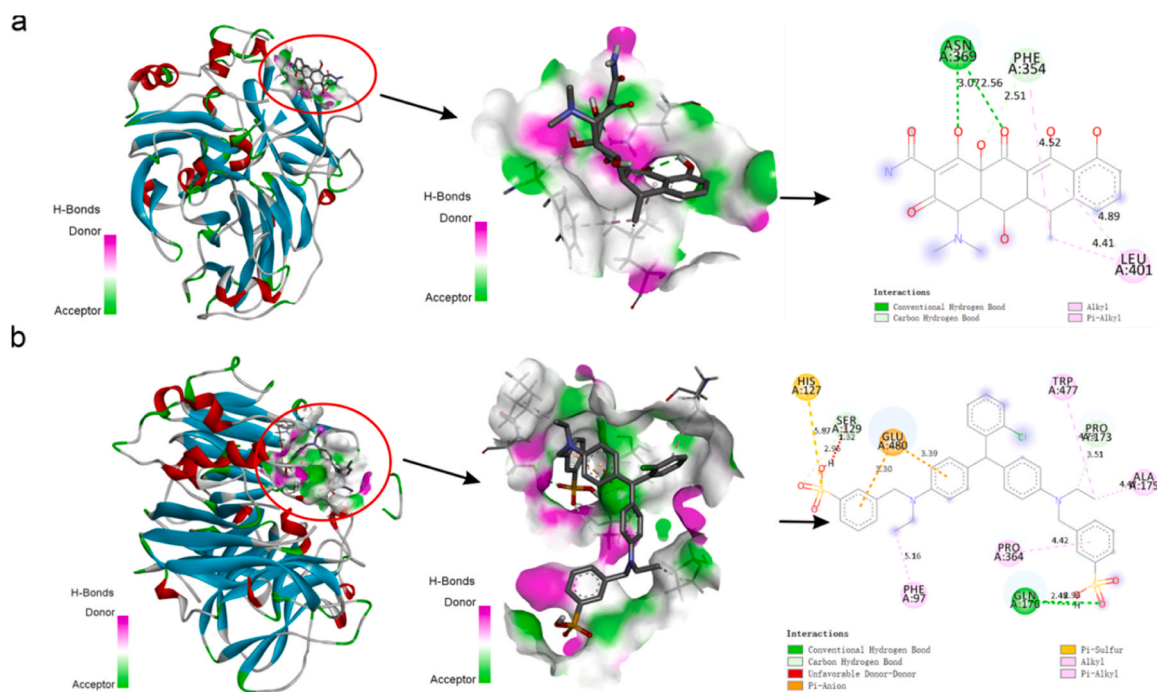


**Fig. 3.** Establishing a molecular docking model for LeLac12 with TET and AG. a, LeLac12 and TET molecular docking model; b, LeLac12 and AG molecular docking model.

and decreased significantly after 4 h of reaction (Fig. S3). Previous studies have shown that mediators have a major impact on the degradation of antibiotics by laccase mediated oxidation (Shao et al., 2019). In the laccase-ABTS and laccase-HBT systems, the degradation rates of TET by LeLac12 were  $79.33 \pm 0.80\%$  and  $97.55 \pm 0.17\%$ , respectively. However, the degradation rate of TET without mediator was only  $47.55 \pm 5.82\%$ . These results suggest that LeLac12 first oxidizes with the mediator to generate active free radicals, which then react with the substrate (Margot et al., 2015).

The metabolites of TET degradation by the LeLac12-HBT system were analyzed by HPLC-ESI-Q-TOF-MS. Mass spectrometry information and possible chemical formulas are listed in Table S7. The possible degradation pathway of TET by the LeLac12-HBT system was speculated

for six metabolic pathways as shown in Fig. 4. Some of degradation products were identified in previous study (Zhang et al., 2019; Han et al., 2023; Sun et al., 2021, 2017; Tang et al., 2021; Xu et al., 2022; Shao et al., 2019; Liu et al., 2018). The degradation products of T1 ( $m/z$  431.17828) and T6 ( $m/z$  417.14352) were described for the first time in this study.

The antimicrobial activity of TET and TET degradation products by LeLac12-HBT treatment was evaluated by growth inhibition of *E. coli* and *B. subtilis*. The two strains hardly grow with TET (Tian et al., 2020). The growth inhibition of *E. coli* and *B. subtilis* by TET was completely lost after 4 h of treatment with the LeLac12-HBT system incubation at  $30^\circ\text{C}$  (Fig. S4a,b). The two strains were separately spread on TET degradation products adding LB plate (Fig. S4c,d), found that TET degradation

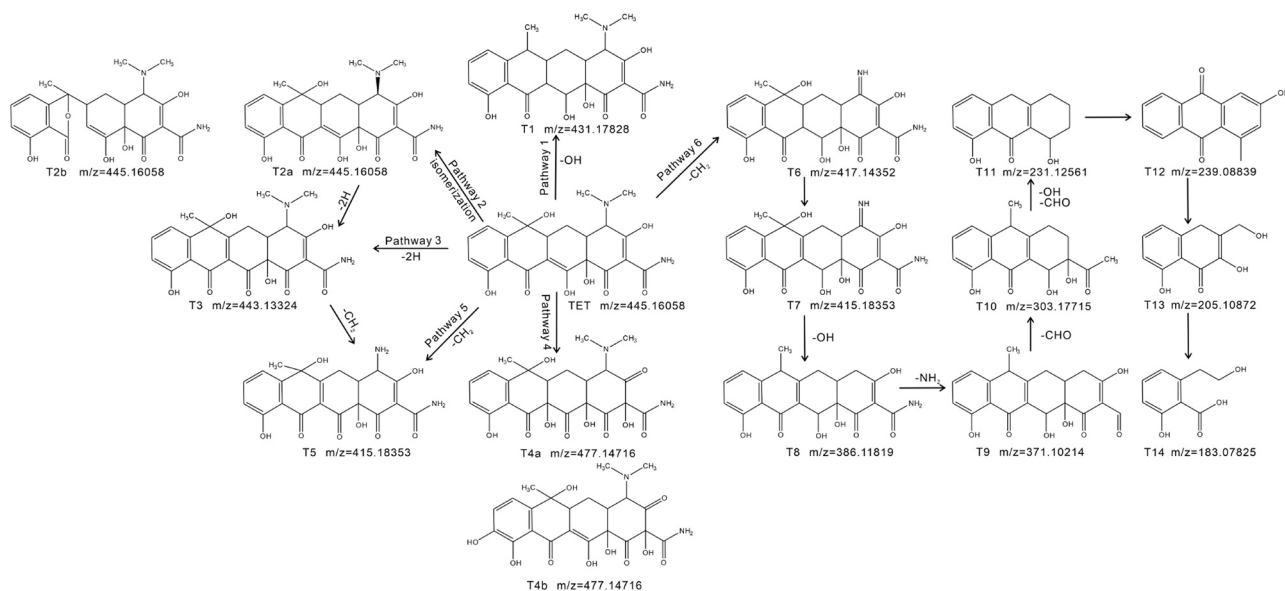


**Fig. 4.** Possible degradation pathway of TET by LeLac12.

products do not have toxic stress on the two strains.

### 3.5. Transformation of AG by LeLac12

The decolorization activity of laccase LeLac12 towards three types of synthetic dyes, anthraquinone, triphenylmethane, and azo dyes, was determined to evaluate its industrial application (Fig S5). LeLac12 had the highest degradation rate against anthraquinone dyes, and the degradation rates of AG, AB-40, AB-KNR were  $93.13 \pm 0.56\%$ ,  $89.11 \pm 0.19\%$ , and  $75.96 \pm 0.11\%$ , respectively (Fig. S5a). AB-KNR and AB-40 were almost completely decolorized while AG was degraded to brown color (Fig. S5b). LeLac12 had lower degradation capacity towards triphenylmethane and azo dyes and the degradation rate was below 20%.

The conditions for decolorization of AG by LeLac12 were optimized and similar results to ABTS oxidation were obtained (Fig. S6). The most suitable pH for AG decolorization was pH 3.0 and the highest degradation rate at different temperatures was observed at 30 °C. The catalytic efficiency of laccase is significantly influenced by the type of mediator (Bhardwaj et al., 2022). In this study, the decolorization rate of AG without mediators was 100%. When ABTS or HBT was added as a mediator, the decolorization percentage of AG was  $97.7 \pm 3.2\%$  and  $95.67 \pm 0.1\%$ , respectively.

Under the best conditions, the degradation rate of LeLac12 to AG varied at different concentrations. At 200–400 mg/L, AG was almost completely degraded by LeLac12. At 4000 mg/L, the decolorization rate still reached 89% within 4 h. LeLac12 maintained its decolorization activity during the long degradation process. Park et al. (2019) reported that the highest decolorization rate of AG by laccase was 48.75%, which was far lower than that of LeLac12. So LeLac12 had a strong degradation ability for AG.

Dyes generally contain chromophores such as  $-C=C-$ ,  $-C=O$ ,  $-N=N-$ ,  $-C-N-$ , etc. The chromophores disappear, the dye decolorizes. The degradation of RhB is mainly due to the destruction of the conjugated structures, whereby the intermediates are converted into acidic molecules and degraded to water and carbon dioxide (He et al., 2009). Acidic molecules have also been detected in LeLac12 degradation of AG, including phthalic acid, phthalic acid anhydride, and benzeneformal acid compounds. 1,2-propanediol was also detected in the AG intermediate. According to GC-MS, the proposed AG degradation pathway by LeLac12 was as follow (Fig. 5): the anthraquinone group first broken into diethyl phthalate, oxidation to open one ring, and benzeneformic acid further transform to 1,2-propanediol for final decolorization.

### 3.6. Synergistically enhanced degrade TET and AG by LeLac12 in the co-contamination system

The catalytic efficiency of laccase is significantly influenced by the type of mediator (Bhardwaj et al., 2022). In this study, the most significant improvement in the degradation of TET by LeLac12 from  $47.55 \pm 5.82\%$  to  $97.55 \pm 0.17\%$  was achieved by adding HBT as a mediator, while the decolorization percentage of AG without mediators was 100%. In the co-contamination system of TET and AG, AG showed positive effects on the degradation of TET by LeLac12. Our results showed that

TET was completely degraded within 4 h regardless of the addition of mediators, and the decolorization of AG was also over 96% (Table S8). These results suggest that AG may act as a mediator for TET, ultimately leading to enhanced degradation of TET, ultimately leading to enhanced degradation of TET.

As shown in Table 1, laccases have been identified from fungi used for the degradation of antibiotics, mainly from *Trametes versicolor* and *Pleurotus ostreatus*. So far, laccase from *L. edodes* has been used in the literature for the degradation of dyes, while there is no report on the use of laccase from *L. edodes* for the degradation of antibiotics. In previous studies, laccase was mostly used for the degradation of antibiotics or dyes. There are few research papers dealing with the degradation of antibiotics and dyes in the system of co-contamination by fungal laccase. The co-contamination of various organic compounds in polluted areas is a major challenge for bioremediation due to the complex inhibitory effect of pollutants. Fungal laccase usually needs to add mediators to degrade pollutants, and the addition of these mediators introduces new pollutants. In addition, laccase reacts in different ways with different mediators, and its environmental toxicity is also different. In the present study, a native laccase from *L. edodes* was used to degrade TET and AG. This result indicates that the laccase LeLac12 from *L. edodes* can be used for the degradation of antibiotics and dyes in complex polluted wastewater.

### 3.7. Safety assessment of the degradation products by proteomic analysis

The toxic effects of degradation intermediates were important factors for the safe use of biocatalysts in bioremediation (Wang et al., 2021). The metabolic response of bacteria was an important indicator for the evaluation of the sample safety and could also help us understand the pollutants-related stress response. Label-free quantitative proteomics was used to study the response of *E. coli* to TET, AG, and the degradation products of these compounds to evaluate the potential biological effects.

A total of 1815 proteins (Dataset S2) were identified in the five groups (TET, TETDeg, AG, AGDeg, and CK), accounting for 41.23% of the total predicted proteins in the *E. coli* genome. 1169 proteins, accounting for 64.41% of the total identified proteins, were detected in all five groups (Fig. 6a, Dataset S3). Principal component analysis (PCA) analysis (Fig. 6c, Dataset S5) showed that the protein expression profile of the TET group had a higher correlation with that of the AG group. The lowest correlation was observed between the TET and TETDeg groups. Similar results were observed in the Pearson correlation analysis (Fig. 6b, Dataset S4). The samples of all groups were reasonable with good correlations between the biological replicates. The results of correlation analysis and PCA were similar, showing that TET, AG, and their degradation products have different stress effects on *E. coli*.

The volcano plots (Fig 6defg) were used to reveal the numerous differentially expressed proteins (DEPs) in *E. coli*. A 2.0-fold change cutoff and a p-value BH < 0.05 were used to categorize the DEPs. Compared to CK, the largest number of DEPs (78 upregulated and 87 down-regulated) was observed when the *E. coli* were grown in the TET group (Dataset S6). The TETDeg group was with 12 upregulated and 38 downregulated proteins. There were 37 upregulated and 111

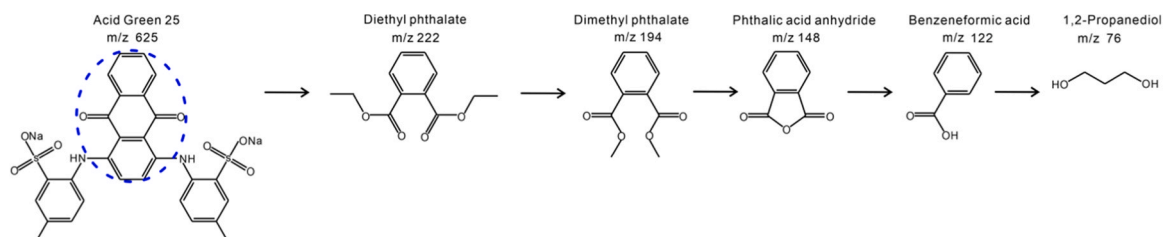


Fig. 5. The proposed degradation pathway of AG by LeLac12 without mediator. The anthraquinone group of AG has been labeled by the blue dotted line.

**Table 1**

Summary of the degradation of TET and dyes by laccase from different strains. Percentages represent the degradation efficiency.

Laccase	Source	Substrate	Degradation efficiency	Toxicity after treatment	Transformation products	Reference
Trametes versicolor IFO 6482	Purified	TET, OTC, CTC, DC	100% after 1 h; (HBT)	Reduced ( <i>Bacillus subtilis</i> and <i>E. coli</i> )	No report	Suda et al., (2012)
Trametes versicolor	Purchased	TET	30% after 24 h with free laccase	No report	[M + H] <sup>+</sup> : TP 461; TP 427.	Cazes et al., (2014)
	Purchased	TET	TET: > 200 mg h <sup>-1</sup> m <sup>-2</sup> for 24 h	No report	No report	Cazes et al., (2015)
	Purchased	TET	TET: 78% after 18 h	Reduced ( <i>Bacillus subtilis</i> ATCC633)	[M + H] <sup>+</sup> : TP 431; TP 396	Llorca et al., (2015)
	Purchased	TET, OTC, DC	85% after 24 h (SYR) OTC: 89% after 24 h	Increased ( <i>Bacillus subtilis</i> ATCC6633 and <i>Aliivibrio fischer</i> )	No report	Becker et al., (2016)
Trametes versicolor	Purchased	TET, OTC	TET: 100% after 3 h OTC: 95% after 3 h	No report	No report	Ding et al., (2016)
<i>Cerrena</i> sp. HYB07	Fermentation broth	TET, OTC	TET, OTC: over 80% after 12 h	Reduced ( <i>Bacillus licheniformis</i> and <i>E. coli</i> )	[M + H] <sup>+</sup> : TP 459; TP 431; TP 396.	Yang et al., (2017)
<i>Pleurotus ostreatus</i>	Purchased	TET	TET: 96% after 6 h (0 mg L <sup>-1</sup> HA); 90% after 6 h (40 mg L <sup>-1</sup> HA)	Reduced ( <i>E. coli</i> )	[M - H] <sup>-</sup> : TP 459; TP 457; TP 429; TP 441; TP 425; TP 394.	Sun et al., (2017)
Trametes versicolor	Purchased	TET	TET: 98% after 3 h (SA); 94% after 3 h (HBT)	No report	[M + H] <sup>+</sup> : TP 431; TP 415; TP 386; TP 371; TP 327.	Shao et al., (2019)
<i>Pycnoporus</i> sp. SYBC-L10	Purified	TET, OTC	TC: 100% after 4 min at 25 °C; 100% after 5 min at 0 °C OTC: 100% after 5 min at 25 °C; 100% after 5 min at 0 °C (ABTS)	Reduced ( <i>Bacillus altitudinis</i> SYBC hb4 and <i>E. coli</i> )	[M + H] <sup>+</sup> : TP 445; TP 431; TP 413; TP 399; TP 381; TP 367; TP 351.	Tian et al., (2020)
<i>Lentinula edodes</i>	Recombinant expressed	MR, RO16, CBBR, BPB, CV, IC, NBB, RBBR	Most dyes have a degradation rate of more than 80%. (TEMPO or HBT)	No report	No report	Wong et al., (2012)
<i>Lentinula edodes</i>	Purified	RBBR, NBB, BPB, CBB	It is not explicitly stated	No report	No report	Nagai et al., (2009)
<i>Lentinula edodes</i>	Purified	indigo dye	40% of dye degradation after 48 h	No report	No report	da Luz et al., (2023)
<i>Fusarium oxysporum</i>	Fermentation broth	malachite green	MG: ≤ 100 mg/L, degradation efficiency ≥ 90% (HBT)	<i>E. Coli</i> ATCC85922	No report	Thoa et al., (2022)
Trametes versicolor	Purchased	malachite green, indigo carmine,	malachite green of 61.30% (A) and of 21.52% in indigo carmine	No report	No report	Haro-Mares et al., (2022)
Trametes versicolor WH21	Purified	Azure B and sulfacetamide	Azure B: 46.8% (HBT); sulfacetamide : 47.5% (HBT)	No report	Sulfacetamide: S1 ( <i>m/z</i> , 229.03), S2 ( <i>m/z</i> , 251.12), S3 ( <i>m/z</i> , 168.11)	Zhang et al., (2023)

downregulated of DEPs in TET vs TETDeg group. Compared with CK group, 65 proteins were upregulated and 25 proteins were down-regulated in AG group (Dataset S7). DEPs between AGDeg group and CK group were less than those between AG group and other groups.

KEGG pathway analysis was performed for the DEPs of each comparison. Biological phenotype was used to indicate the toxicity of environmental pollutants (Yu et al., 2019a). Proteomics was used to describe the biological phenotype caused by intermediates on the expression and translation of the *Vibrio fischeri luminescence* gene (Antonopoulou et al., 2016). The TET-up DEPs were associated with specific KEGG pathways, which were mainly distributed in biosynthesis of secondary metabolites, carbon metabolism, pyruvate metabolism, glycolysis/gluconeogenesis, Mismatch repair, Homologous recombination, DNA replication, citrate cycle, RNA polymerase, nucleotide exception repair (Fig. 7). Pyruvate metabolism and citrate cycle were upregulated, indicating that *E. coli* will produce more energy in facing TET stress, providing sufficient electrons for TET degradation (Sun et al., 2019). The down-regulation pathway included metallic pathways, ribome, biosynthesis of cofactors, biosynthesis of amino acid, nicotinate and nicotinamide metabolism, fatty acid biosynthesis etc.

TET inhibited protein synthesis by blocking the binding of aminoacylated tRNA and 30 S subunit A site. The ribosome is an important target of many antibiotics (Pioletti et al., 2001; Brodersen et al., 2000). The large subunit ribosomal protein S17, L24, L5, and L30 of Ribosomes were downregulated, reducing the synthesis of protein, RNA, and DNA in *E. coli* (Yu et al., 2019b).

Bacteria produce cofactors to catalyze the degradation of pollutants. The synthesis of cofactors could effectively help bacteria to cope with a stressful environment (Mahendran et al., 2019). Coenzyme played an important role in the tricarboxylic acid cycle, and the deficiency of coenzyme A inhibited the growth of the strain. The effects of these metabolic pathways were related to the inhibition of *E. coli* cell growth by antibiotics (Lobritz et al., 2015). KEGG analysed TET inhibits the growth of *E. coli* by inhibiting the transcription, translation, and other energy supplies. The up-regulation of beta lactam resistance and bacterial chemotaxis indicated that TET has more toxic, confirming that LeLac12 can degrade toxic TET into non-toxic compounds. Benzoate degradation is the main pathway for microorganisms to decompose various polycyclic aromatic hydrocarbons (Yadav et al., 2020), which was downregulated in both groups. Tyrosine metabolism, nucleotide

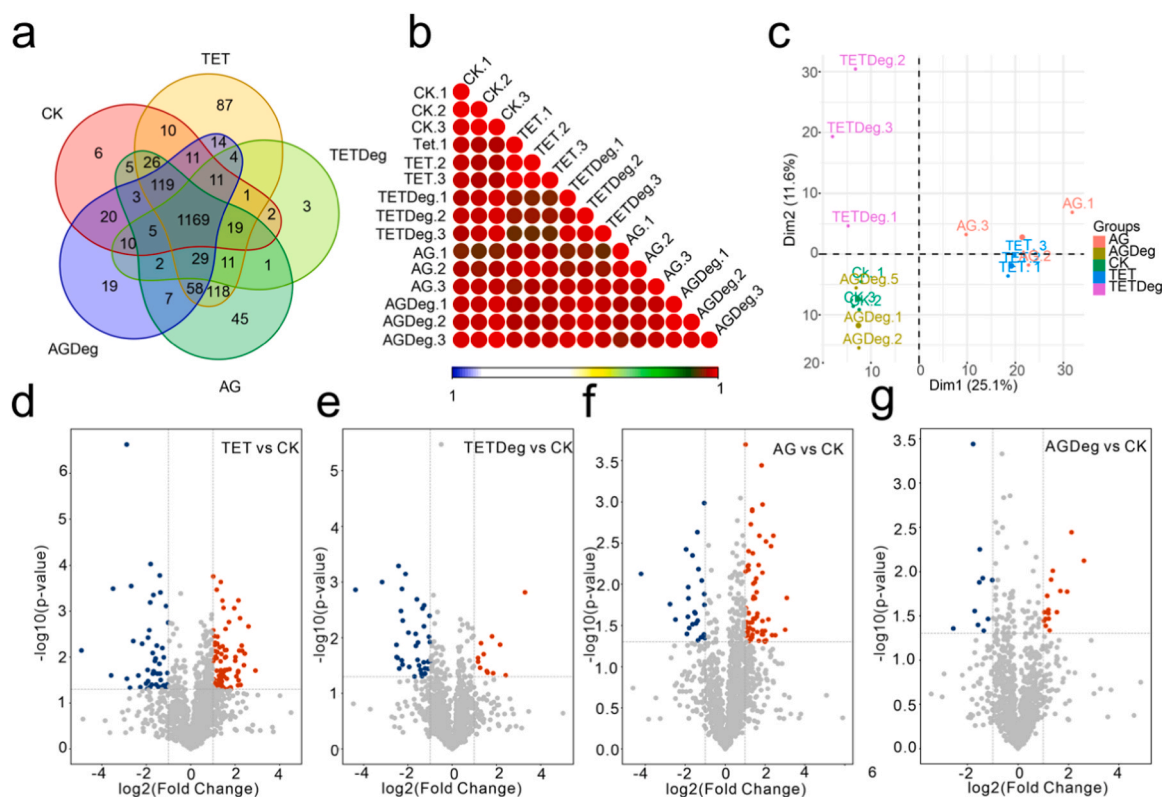


**Fig. 6.** Detection of stress difference between TET and its degradation products, AG and its degradation products on *E. coli* by proteome technology. a, The amount of protein in *E. coli* detected in TET, TETDeg, AG, AGDeg, CK groups; b, Correlation between TET, TETDeg, AG, AGDeg, and CK groups; c, Principal component analysis of TET, TETDeg, AG, AGDeg, CK groups; d, Difference expression of *E. coli* intracellular protein in TET and CK; e, Difference expression of *E. coli* intracellular protein in TETDeg and CK; f, Difference expression of *E. coli* intracellular protein in AG and CK; g, The difference between *E. coli* intracellular protein in AGDeg and CK: red indicates the upregulated protein, blue indicates the downregulated protein, and gray indicates the common protein of the two groups.

exception repair, novobiocin biosynthesis, monobactam biosynthesis, histidine metabolism down-regulation pathways were only present in the TET group. In TETDeg group, there were only 7 upregulated pathways, with only 2 proteins upregulated in addition to Metabolic Pathways, and only 1 protein upregulated in the Two-component system. Down-regulation of quorum sensing can significantly reduce the expression of pathogenic genes and drug resistance genes, but has no effect on the growth of microorganisms. Two-component system played an important role in signal transduction (Moreira et al., 2019). The down-regulation pathways mainly focus on ABC transporters, quorum sensing, pyruvate metabolism, beta Lactam resistance, and bacterial chemotaxis. TET mainly affects the RNA transcription and protein translation process of cells, and metabolites mainly affects the carbon metabolism and amino acid synthesis. TET and its metabolites by LeLac12 had different stress effects on *E. coli*.

In the AG group, the upregulated pathway was found to be mainly involved in carbon metabolism (Fig. 8), which means that *E. coli* produces a large amount of energy when confronted with anthraquinone dyes (Zhang et al., 2022), and the downregulated protein was involved in the Pentose phase pathway, Oxidative photosynthesis, Lipopolysaccharide biosynthesis, Glycerolide metabolism and amino acid metabolism pathways, amino acid metabolism pathways. The upregulated pathway was accompanied by the production of ATP, which provides energy for the growth and metabolism of *E. coli*.

To determine the functions of these DEPs, GO enrichment analysis was performed to classify the annotated DEPs for each comparison (Fig. S7 and Fig. S8). Compared with the CK group, the upregulated DEPs in TET and TETDeg groups were enriched in the Biological Process (BP) category while the downregulated DEPs had the least terms in Molecular Function (MF). In the comparison between TETDeg and CK, in TETDeg group only 6 upregulated and 61 downregulated DEPs were

assigned in GO terms, including 13 BP, 4 Cellular Component (CC), and 1 MF terms. In the comparison of AG vs CK, 65 upregulated and 25 downregulated DEPs were assigned in GO terms, including 24 BP, 7 CC, and 19 MF terms. In the comparison of AGDeg vs CK, 17 upregulated and 10 downregulated DEPs, no DEPs could be assigned to three GO terms. TET and AG induced upregulated and downregulated DEPs in the proteome of *E. coli* with different terms in all three GO categories. TET mainly affected BP function, after treat with LeLac12 the products mainly conducted the change in BP function. AG took an overall effect, while the degradation products of AG do not have a significant impact on the growth of *E. coli*. Through GO enrichment analysis, we have found that the translation process of *E. coli* is affected in the presence of AG and TET. The impact of the degradation products on *E. coli* growth primarily lies in energy metabolism processes such as transport and oxidoreductase activity. These results provide important insights into the response mechanisms of *E. coli* to pollutants and their metabolites and confirm the detoxification ability of LeLac12 against toxic pollutants.

#### 4. Conclusions

The laccase secreted by the white rot fungus *L. edodes* to degrade TET and dyes was identified for the first time. The recombinantly expressed laccase showed different abilities to degrade TET and dyes. It is important to emphasize that we succeeded in identifying the degradation products of TET and AG separately. Growth inhibition of *E. coli* and *B. subtilis* showed that the antimicrobial activity of TET was significantly reduced after treatment with the laccase-HBT system. Proteomic analysis revealed that TET could affect the central carbon metabolism and energy metabolism system of *E. coli* and induce the expression of proteins related to DNA replication and repair, which could be one of the

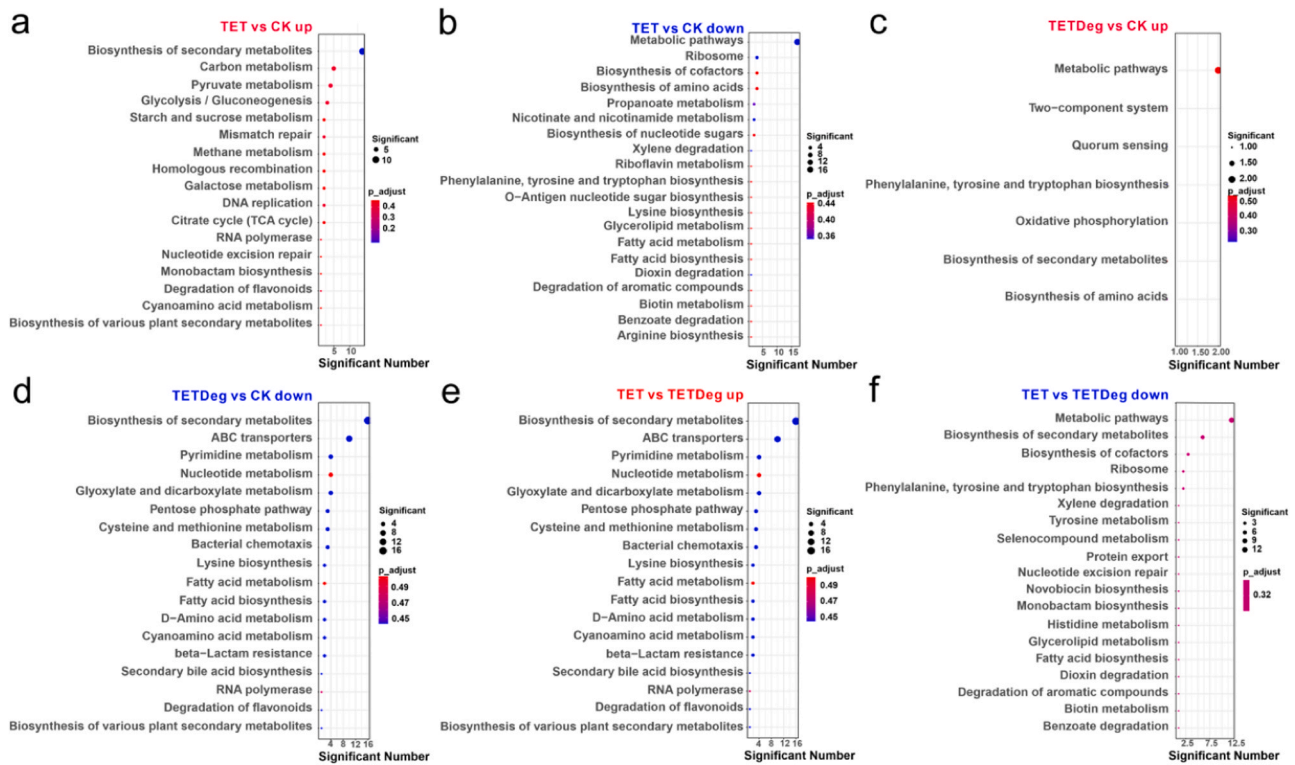


**Fig. 7.** Enriched KEGG terms of differentially expressed proteins in TET and TETDeg groups compared with the CK group in *E.coli*. Circle size indicates protein counts. The circle color indicates the p-value. a, Enriched analysis of upregulated proteins between TET and CK; b, Enriched analysis of downregulated proteins between TET and CK; c, Enriched analysis of upregulated proteins between TETDeg and CK; d, Enriched analysis of downregulated proteins between TETDeg and CK; e, Enriched analysis of upregulated proteins between TET and TETDeg; f, Enriched analysis of downregulated proteins between TET and TETDeg.

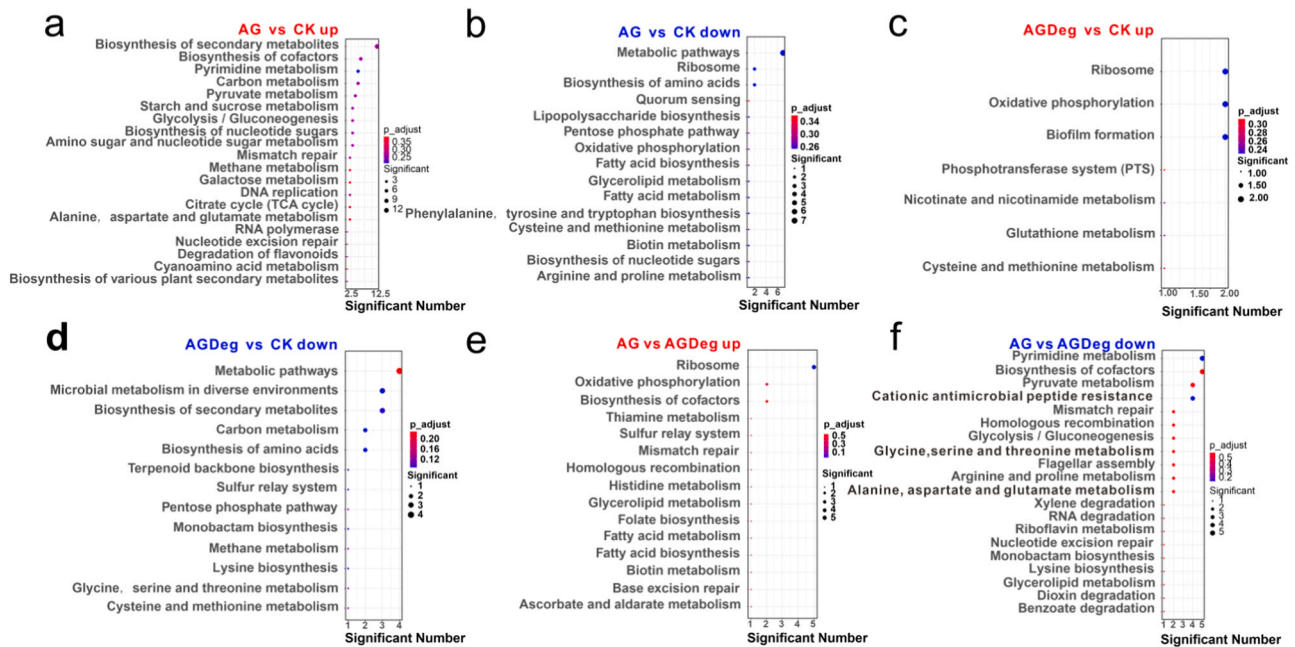


**Fig. 8.** Enriched KEGG terms of differentially expressed proteins in AG and AGDeg groups compared with the CK group in *E.coli*. Circle size indicates protein counts. The circle color indicates the p-value. a, Enriched analysis of upregulated proteins between AG and CK; b, Enriched analysis of downregulated proteins between AG vs CK; c, Enriched analysis of upregulated proteins between AGDeg and CK; d, Enriched analysis of downregulated proteins between AGDeg and CK; e, Enriched analysis of upregulated proteins between AG and AGDeg; f, Enriched analysis of downregulated proteins between AG and AGDeg.

factors inducing the formation of multidrug-resistant strains. The ability of LeLac12 to degrade TET was significantly enhanced by the addition of AG. This study demonstrated the bioremediation effect of laccase on the co-

contamination system of TET and AG and provided experimental support for the application of laccase in the treatment of complex polluted wastewater.

## Funding

This work was supported by the Key R&D Program of Shandong Province (2022LZGC023), Shandong Edible Fungus Agricultural Technology System (SDAIT-07-02), and Qingdao Agricultural University Doctoral Start-Up Fund (663/1119047).

## CRediT authorship contribution statement

**Shuxue Zhao:** Writing – original draft, Visualization, Investigation, Data curation. **Xiaohang Li:** Visualization, Data curation. **Xingdong Yao:** Data curation. **Xuyang Liu:** Writing – review & editing. **Chao Pan:** Methodology. **Lizhong Guo:** Funding acquisition. **Jie Bai:** Conceptualization. **Tiantian Chen:** Investigation. **Hao Yu:** Writing – review & editing, Data curation, Conceptualization. **Chunhui Hu:** Writing – review & editing, Funding acquisition, Data curation, Conceptualization.

## Declaration of Generative AI and AI-assisted technologies in the writing process

The authors declare that they did not use generative AI and AI-assisted technologies in the writing process.

## Declaration of Competing Interest

The authors declare the following financial interests/personal relationships which may be considered as potential competing interests: Hao Yu, Chunhui Hu, Jingtian Hu, Shuxue Zhao has patent pending to 2023104452844. If there are other authors, they declare that they have no known competing financial interests or personal relationships that could have appeared to influence the work reported in this paper.

## Data availability

Data will be made available on request.

## Acknowledgments

We thank the Instrumental Analysis Center of Qingdao Agricultural University and Central Laboratory of the School of Life Science. We also thank Lin Song and Zhijuan Sun for providing technical support.

## Appendix A. Supporting information

Supplementary data associated with this article can be found in the online version at [doi:10.1016/j.ecoenv.2024.116324](https://doi.org/10.1016/j.ecoenv.2024.116324).

## References

- Adak, A., Tiwari, R., Singh, S., Sharma, S., Nain, L., 2016. Laccase production by a novel White-Rot Fungus *Pseudolagarobasidium acaciicola* LA 1 through solid-state fermentation of *Parthenium* biomass and its application in dyes decolorization. *Waste Biomass. Valoriz.* 7, 1427–1435. <https://doi.org/10.1007/s12649-016-9550-0>.
- Antonopoulou, M., Karagianni, P., Konstantinou, I.K., 2016. Kinetic and mechanistic study of photocatalytic degradation of flame retardant Tris (1-chloro-2-propyl) phosphate (TCPP). *Appl. Catal. B-Environ.* 192, 152–160. <https://doi.org/10.1016/j.apcatb.2016.03.039>.
- Becker, D., Varela Della Giustina, S., Rodríguez-Mozaz, S., Schoevaart, R., Barceló, D., de Cazes, M., Belleville, M., Sánchez-Marcano, J., de Gunzburg, J., Couillerot, O., Völker, J., Oehlmann, J., Wagner, M., 2016. Removal of antibiotics in wastewater by enzymatic treatment with fungal laccase - Degradation of compounds does not always eliminate toxicity. *Bioresour. Technol.* 219, 500–509. <https://doi.org/10.1016/j.biortech.2016.08.004>.
- Bhagat, C., Kumar, M., Tyagi, V.K., Mohapatra, P.K., 2020. Proclivities for prevalence and treatment of antibiotics in the ambient water: a review. *Clean Water* 1–18. <https://doi.org/10.1038/s41545-020-00087-x>.
- Bhardwaj, P., Kaur, N., Selvaraj, M., Ghramh, H.A., Al-Shehri, B.M., Singh, G., Arya, S.K., Bhatt, K., Ghotekar, S., Mani, R., Woong Chang, S., Ravindran, B., Kumar Awasthi, M., 2022. Laccase-assisted degradation of emerging recalcitrant compounds – a review. *Bioresour. Technol.*, 128031 <https://doi.org/10.1016/j.biortech.2022.128031>.
- Biasini, M., Bienert, S., Waterhouse, A., Arnold, K., Studer, G., Schmidt, T., Kiefer, F., Gallo Cassarino, T., Berton, M., Bordoli, L., Schwede, T., 2014. SWISS-MODEL: modelling protein tertiary and quaternary structure using evolutionary information. *Nucleic Acids Res.* 42, W252–W258. <https://doi.org/10.1093/nar/gku340>.
- Blánquez, A., Rodríguez, J.F., Brissos, V., Mendes, S., Martins, L.O., Ball, A.S., Arias, M. E., Hernández, M., 2018. Decolorization and detoxification of textile dyes using a versatile *Streptomyces* laccase-natural mediator system. *Saudi J. Biol. Sci.* 26, 913–920. <https://doi.org/10.1016/j.sjbs.2018.05.020>.
- Brodersen, D.E., Clemons, W.M., Clemons, W.M., Carter, A.P., Morgan-Warren, R.J., Wimberly, B.T., Ramakrishnan, V., 2000. The structural basis for the action of the antibiotics tetracycline, pactamycin, and hygromycin B on the 30S ribosomal subunit. *Cell* 103, 1143–1154. [https://doi.org/10.1016/s0092-8674\(00\)00216-6](https://doi.org/10.1016/s0092-8674(00)00216-6).
- Cai, Y., Gong, Y., Liu, W., Hu, Y., Chen, L., Yan, L., Yan, L., Y., Bian, Y., 2017. Comparative secretomic analysis of lignocellulose degradation by *Lentinula edodes* grown on microcrystalline cellulose, lignosulfonate and glucose. *J. Proteom.* 163, 92–101. <https://doi.org/10.1002/pmic.201800220>.
- Cazes, M.D., Belleville, M., Mougel, M., Kellner, H.M., Sánchez-Marcano, J., 2015. Characterization of laccase-grafted ceramic membranes for pharmaceuticals degradation. *J. Membr. Sci.* 476, 384–393. <https://doi.org/10.1016/j.memsci.2014.11.044>.
- Cazes, M.D., Belleville, M., Petit, E., Llorca, M., Rodríguez-Mozaz, S., Gunzburg, J.D., Barceló, D., Sánchez-Marcano, J., 2014. Design and optimization of an enzymatic membrane reactor for tetracycline degradation. *Catal. Today* 236, 146–152. <https://doi.org/10.1016/j.cattod.2014.02.051>.
- Chen, L., Gong, Y., Cai, Y., Liu, W., Zhou, Y., Xiao, Y., Xu, Z., Liu, Y., Lei, X., Wang, G., Guo, M., Ma, X., Bian, Y., 2016. Genome sequence of the edible cultivated mushroom *Lentinula edodes* (Shiitake) reveals insights into lignocellulose degradation. *PLOS One* 11, e0160336. <https://doi.org/10.1371/journal.pone.0160336>.
- Chen, X., Li, Y., Zhang, H., Liu, J., Xie, Z., Lin, L., Wang, D., 2018. Quantitative Proteomics reveals common and specific responses of a marine diatom *Thalassiosira pseudonana* to different macronutrient deficiencies. *Front. Microbiol.* 9, 2761. <https://doi.org/10.3389/fmicb.2018.02761>.
- Chen, C., Wu, Y., Li, J., Wang, X., Zeng, Z., Xu, J., Liu, Y., Feng, J., Chen, H., He, Y., Xia, R., 2023. TBools-II: A "one for all, all for one" bioinformatics platform for biological big-data mining. *Mol. Plant* 16, 1733–1742. <https://doi.org/10.1016/j.molp.2023.09.010>.
- Davies, G.J., Williams, S.J., 2016. Carbohydrate-active enzymes: sequences, shapes, connotations and cells. *Biochem. Soc. Trans.* 44, 79–87. <https://doi.org/10.1042/BST20150186>.
- Ding, H., Wu, Y., Zou, B., Lou, Q., Zhang, W., Zhong, J., Lu, L., Dai, G., 2016. Simultaneous removal and degradation characteristics of sulfonamide, tetracycline, and quinolone antibiotics by laccase-mediated oxidation coupled with soil adsorption. *J. Hazard Mater.* 307, 350–358. <https://doi.org/10.1016/j.jhazmat.2015.12.062>.
- Drula, E., Garron, M.L., Dogan, S., Lombard, V., Henrissat, B., Terrapon, N., 2022. The carbohydrate-active enzyme database: functions and literature. *Nucleic Acids Res.* 50, D571–D577. <https://doi.org/10.1093/nar/gkab1045>.
- García-Delgado, C., Eymar, E., Camacho-Arévalo, R., Petruccioli, M., Crognale, S., D'Annibale, A., 2018. Degradation of tetracyclines and sulfonamides by stevensite- and biochar-immobilized laccase systems and impact on residual antibiotic activity. *J. Chem. Technol. Biotechnol.* 93, 3394–3409. <https://doi.org/10.1002/jctb.5697>.
- Giardina, P., Faraco, V., Pezzella, C., Piscitelli, A., Vanhulle, S., Sannia, G., 2010. Laccases: a never-ending story. *Cell. Mol. Life Sci.* 67, 369–385. <https://doi.org/10.1007/s00018-009-0169-1>.
- Gui, W., Lin, J., Liang, Y., Qu, Y., Zhang, L., Zhang, H., Li, X., 2019. A two-step strategy for high-efficiency fluorescent dye removal from wastewater. *npj Clean. Water* 2, 16. <https://doi.org/10.1038/s41545-019-0041-2>.
- Han, Z., Wang, H., Zheng, J., Wang, S., Yu, S., Lu, L., 2023. Ultrafast synthesis of laccase-copper phosphate hybrid nanoflowers for efficient degradation of tetracycline antibiotics. *Environ. Res.* 216, 114690 <https://doi.org/10.1016/j.envres.2022.114690>.
- Haro-Mares, N.B., Meza-Contreras, J.C., López-Dellamary, F.A., Richaud, A., Méndez, F., Curiel-Olague, B.G., Buntkowsky, G., Manríquez-González, R., 2022. Lysine functionalized cellulose for a zwitterion-based immobilization of laccase enzyme and removal of commercial dyes from aqueous media. *Surf. Interfaces* 35, 102412. <https://doi.org/10.1016/j.surfint.2022.102412>.
- Hartmann, E.M., Armengaud, J., 2014. Shotgun proteomics suggests involvement of additional enzymes in dioxin degradation by *Sphingomonas wittichii* RW1. *Environ. Microbiol.* 16, 162–176. <https://doi.org/10.1111/1462-2920.12264>.
- He, Z., Yang, S., Ju, Y., Sun, C., 2009. Microwave photocatalytic degradation of *Rhodamine B* using TiO<sub>2</sub> supported on activated carbon: mechanism implication. *J. Environ. Sci.* 21, 268–272. [https://doi.org/10.1016/s1001-0742\(08\)62262-7](https://doi.org/10.1016/s1001-0742(08)62262-7).
- Hori, C., Gaskell, J., Igarashi, K., Kersten, P., Mozuch, P., Samejima, M., Cullen, D., 2014. Temporal alterations in the secretome of the selective ligninolytic fungus *Ceriporiopsis subvermiformis* during growth on aspen wood reveal this organism's strategy for degrading lignocellulose. *Appl. Environ. Microb.* 80, 2062–2070. <https://doi.org/10.1128/aem.03652-13>.
- Huang, X., Zhang, R., Qiu, Y., Wu, H., Xiang, Q., Yu, X., Zhao, K., Zhang, X., Chen, Q., Penttinen, P., Gu, Y., 2020. RNA-seq profiling showed divergent carbohydrate-active enzymes (CAZymes) expression patterns in *Lentinula edodes* at brown film formation stage under blue light induction. *Front. Microbiol.* 11, 1044. <https://doi.org/10.3389/fmicb.2020.01044>.
- Iark, D., Buzzo, A.J.D.R., Garcia, J.A.A., Córreac, V.G., Helmd, C.V., Corrêac, R.C.G., Peraltae, R.A., Moreiraf, R.F.P.M., Peralta, A.B.R.M., 2019. Enzymatic degradation and detoxification of azo dye Congo red by a new laccase from *Oudemansiella canarii*. *Bioresour. Technol.* 289, 121655 <https://doi.org/10.1016/j.biortech.2019.121655>.

- Jain, S.N., Gogate, P.R., 2018. Efficient removal of acid green 25 dye from wastewater using activated *Prunus dulcis* as biosorbent: batch and column studies. *J. Environ. Manag.* 210, 226–238. <https://doi.org/10.1016/j.jenvman.2018.01.008>.
- Jeon, S.J., Lim, S.J., 2017. Purification and characterization of the laccase involved in dye decolorization by the White-Rot Fungus *Marasmius scorodonius*. *J. Microbiol. Biotechnol.* 27, 1120–1127. <https://doi.org/10.4014/jmb.1701.01004>.
- Khan, S., Malik, A., 2014. Environmental and health effects of textile industry wastewater. *Environ. Deterior. Hum. Health* 55–71. [https://doi.org/10.1007/978-94-007-7890-0\\_4](https://doi.org/10.1007/978-94-007-7890-0_4).
- Kishor, R., Purchase, D., Saratale, G.D., Saratale, R.G., Ferreira, L.F.R., Bilal, M., Bharagava, R.N., 2021. Ecotoxicological and health concerns of persistent coloring pollutants of textile industry wastewater and treatment approaches for environmental safety. *J. Environ. Chem. Eng.* 9, 105012. <https://doi.org/10.1016/j.jece.2020.105012>.
- Lee, K., Kalyani, D.C., Tiwari, M.K., Kim, T., Dhiman, S.S., Lee, J., Kim, I., 2012. Enhanced enzymatic hydrolysis of rice straw by removal of phenolic compounds using a novel laccase from yeast *Yarrowia lipolytica*. *Bioresour. Technol.* 123, 636–645. <https://doi.org/10.1016/j.biortech.2012.07.066>.
- Levasseur, A., Drula, E., Lombard, V., Coutinho, P.M., Henrissat, B., 2013. Expansion of the enzymatic repertoire of the CAZy database to integrate auxiliary redox enzymes. *Biotechnol. Biofuels* 6, 41. <https://doi.org/10.1186/1754-6834-6-41>.
- Li, Z., Nandakumar, R., Madayiputhiya, N., Li, X., 2012. Proteomic analysis of 17 $\beta$ -estradiol degradation by *Stenotrophomonas maltophilia*. *Environ. Sci. Technol.* 46, 5947–5955. <https://doi.org/10.1021/es300273k>.
- Liu, Y., Kong, J., Yuan, J., Zhao, W., Zhu, X., Sun, C., Xie, J., 2018. Enhanced photocatalytic activity over flower-like sphere Ag/Ag<sub>2</sub>CO<sub>3</sub>/BiVO<sub>4</sub> plasmonic heterojunction photocatalyst for tetracycline degradation. *Chem. Eng. J.* 331, 242–254. <https://doi.org/10.1016/j.cej.2017.08.114>.
- Liu, C., Zhang, W., Qu, M., Pan, K., Zhao, X., 2020. Heterologous expression of laccase from *Lentinula edodes* in *Pichia pastoris* and its application in degrading rape straw. *Front. Microbiol.* 11. <https://doi.org/10.3389/fmicb.2020.01086>.
- Llorca, M., Rodríguez-Mozaz, S., Coullierot, O., Panigoni, K., de Gunzburg, J., Bayer, S., Czaja, R., Barceló, D., 2015. Identification of new transformation products during enzymatic treatment of tetracycline and erythromycin antibiotics at laboratory scale by an on-line turbulent flow liquid-chromatography coupled to a high resolution mass spectrometer LTQ-Orbitrap. *Chemosphere* 119, 90–98. <https://doi.org/10.1016/j.chemosphere.2014.05.072>.
- Lobritz, M.A., Belenky, P., Porter, C.B., Gutierrez, A., Yang, J.H., Schwarz, E.G., Dwyer, D.J., Khalil, A.S., Collins, J.J., 2015. Antibiotic efficacy is linked to bacterial cellular respiration. *P. Natl. Acad. Sci. USA* 112, 8173–8180. <https://doi.org/10.1073/pnas.1509743112>.
- da Luz, J.M.R., de Souza Lopes, L., da Silva, M.C.S., Vieira, N.A., Cardoso, W.S., Kasuya, M.C.M., 2023. *Lentinula edodes* lignocellulolases and lipases produced in Macaíba residue and use of the enzymatic extract in the degradation of textile dyes. *BioTech* 13 (12), 406. <https://doi.org/10.1007/s13205-023-03827-1>.
- Mahajan, S., Master, E.R., 2010. Proteomic characterization of lignocellulose-degrading enzymes secreted by *Phanerochaete carmosa* grown on spruce and microcrystalline cellulose. *Appl. Microbiol. Biotechnol.* 86, 1903–1914. <https://doi.org/10.1007/s00253-010-2516-4>.
- Mahendran, R., Bs, S., Thandeeswaran, M., kG, K., Vijayasathary, M., Angayarkanni, J., Muthusamy, G., 2019. Microbial (enzymatic) degradation of cyanide to produce pterins as cofactors. *Curr. Microbiol.* 77, 578–587. <https://doi.org/10.1007/s00284-019-01694-9>.
- Margot, J., Copin, P.J., von Gunten, U., Barry, D.A., Holliger, C., 2015. Sulfamethoxazole and isoproturon degradation and detoxification by a laccase-mediator system: influence of treatment conditions and mechanistic aspects. *Biochem. Eng. J.* 103, 47–59. <https://doi.org/10.1016/j.bej.2015.06.008>.
- Mitra, S., Sil, A., Biswas, R., Chakrabarty, S., 2023. Molecular thermodynamic origin of substrate promiscuity in the enzyme laccase: Toward a broad-spectrum degrader of dye effluents. *J. Phys. Chem. Lett.* 14 (7), 1892–1898. <https://doi.org/10.1021/acs.jpclett.2c03126>.
- Morales-Álvarez, E.D., Rivera-Hoyos, C.M., Poveda-Cuevas, S.A., Reyes-Guzmán, E.A., Pedrosa-Rodríguez, A.M., Reyes-Montaño, E.A., Poutou-Piñales, R.A., 2018. Malachite green and crystal violet decolorization by *Ganoderma lucidum* and *Pleurotus ostreatus* supernatant and by rGLCC1 and rPOXA 1B concentrates: molecular docking analysis. *Appl. Biochem. Biotechnol.* 184, 794–805. <https://doi.org/10.1007/s12010-017-2560-y>.
- Moreira, L.F., Zomer, S., Marques, S.M., 2019. Modulation of the multixenobiotic resistance mechanism in *Danio rerio* hepatocyte culture (ZF-L) after exposure to glyphosate and roundup. *Chemosphere* 228, 159–165. <https://doi.org/10.1016/j.chemosphere.2019.04.140>.
- Nagai, M., Sakamoto, Y., Nakade, K., Sato, T., 2009. Purification of a novel extracellular laccase from solid-state culture of the edible mushroom *Lentinula edodes*. *Mycoscience* 50, 308–312. <https://doi.org/10.1007/s10267-008-0478-5>.
- Park, J.H., Kim, W., Lee, Y.S., Kim, J.H., 2019. Decolorization of acid green 25 by surface display of CotA laccase on *Bacillus subtilis* spores. *J. Microbiol. Biotechnol.* 29, 1383–1390. <https://doi.org/10.4014/jmb.1907.07019>.
- Paysan-Lafosse, T., Blum, M., Chuguransky, S., Grego, T., Pinto, B.L., Salazar, G.A., Bileschi, M.L., Bork, P., Bridge, A., Colwell, L., Gough, J., Haft, D.H., Letunic, I., Marchler-Bauer, A., Mi, H., Natale, D.A., Orengo, C.A., Pandurangan, A.P., Rivoire, C., Sigrist, C.J.A., Sillitoe, I., Thanki, N., Thomas, P.D., Tosatto, S.C.E., Wu, C., Bateman, A., 2022. InterPro in 2022. *Nucleic Acids Res.* 51 (D1), D418–D427. <https://doi.org/10.1093/nar/gkac993>.
- Pioletti, M., Schlünzen, F., Harms, J.M., Zarivach, R., Glühmann, M., Avila, H., Bashan, A., Bartels, H., Auerbach, T., Jacobi, C., Hartsch, T., Yonath, A.E., Franceschi, F., 2001. Crystal structures of complexes of the small ribosomal subunit with tetracycline, edeine and IF3. *EMBO J.* 20, 1829–1839. <https://doi.org/10.1093/emboj/20.8.1829>.
- Shao, B.B., Liu, Z.F., Zeng, G.M., Liu, Y., Yang, X., Zhou, C.Y., Chen, M., Liu, Y.J., Jiang, Y.L., Yan, M., 2019. Immobilization of laccase on hollow mesoporous carbon nanospheres: noteworthy immobilization, excellent stability and efficacious for antibiotic contaminants removal. *J. Hazard. Mater.* 362, 318–326. <https://doi.org/10.1016/j.jhazmat.2018.08.069>.
- Singh, Z., Chadha, P., 2016. Textile industry and occupational cancer. *J. Occup. Med. Toxicol.* 11, 1–6. <https://doi.org/10.1186/s12995-016-0128-3>.
- Solanki, K., Subramanian, S., Basu, S., 2013. Microbial fuel cells for azo dye treatment with electricity generation: a review. *Bioresour. Technol.* 131, 564–571. <https://doi.org/10.1016/j.biortech.2012.12.063>.
- Song, G., Hsu, Y.P., Walley, J.W., 2018. Assessment and refinement of sample preparation methods for deep and quantitative plant proteome profiling. *Proteomics* 18, 1800220. <https://doi.org/10.1002/pmic.201800220>.
- Songulashvili, G., Elisashvili, V., Wasse, S., Nevo, E., Hadar, Y., 2006. Laccase and manganese peroxidase activities of *Phellinus robustus* and *Ganoderma adspersum* grown on food industry wastes in submerged fermentation. *Biotechnol. Lett.* 28, 1425–1429. <https://doi.org/10.1007/s10529-006-9109-4>.
- Suda, T., Hata, T., Kawai, S., Okamura, H., Nishida, T., 2012. Treatment of tetracycline antibiotics by laccase in the presence of 1-hydroxybenzotriazole. *Bioresour. Technol.* 103, 498–501. <https://doi.org/10.1016/j.biortech.2011.10.041>.
- Sun, X., Bai, R., Zhang, Y.H., Wang, Q., Fan, X., Yuan, J., Cui, L., Wang, P., 2013. Laccase-catalyzed oxidative polymerization of phenolic compounds. *Appl. Biochem. Biotechnol.* 171, 1673–1680. <https://doi.org/10.1007/s12010-013-0463-0>.
- Sun, K., Huang, Q., Li, S., 2017. Transformation and toxicity evaluation of tetracycline in humic acid solution by laccase coupled with 1-hydroxybenzotriazole. *J. Hazard. Mater.* 331, 182–188. <https://doi.org/10.1016/j.jhazmat.2017.02.058>.
- Sun, X.A., Leng, Y., Wan, D., Chang, F., Huang, Y., Li, Z., Xiong, W., Wang, J., 2021. Transformation of tetracycline by manganese peroxidase from *Phanerochaete chrysosporium*. *Molecules* 26, 6803. <https://doi.org/10.3390/molecules26226803>.
- Sun, Q., Sun, Y., Zhang, J., Luan, Z., Lian, C., Liu, S., Yu, C., 2019. High temperature-induced proteomic and metabolomic profiles of a thermophilic *Bacillus manuseusis* isolated from the deep-sea hydrothermal field of Manus Basin. *J. Proteom.* 203, 103380. <https://doi.org/10.1016/j.jpro.2019.103380>.
- Tang, Y., Li, W., Muhammad, Y., Jiang, S., Huang, M., Zhang, H., Zhao, Z., 2021. Fabrication of hollow covalent-organic framework microspheres via emulsion-interfacial strategy to enhance laccase immobilization for tetracycline degradation. *Chem. Eng. J.* 421, 129743. <https://doi.org/10.1016/j.cej.2021.129743>.
- Thoa, L.T.K., Thao, T.T.P., Hung, N.B., Khoo, K.S., Quang, H.T., Lan, T.T., Hoang, V.D., Park, S.M., Ooi, C.W., Show, P.L., Huy, N.D., 2022. Biodegradation and detoxification of Malachite Green dye by extracellular laccase expressed from *Fusarium oxysporum*. *Waste Biomass Valor* 13, 2511–2518. <https://doi.org/10.1007/s12649-022-01692-2>.
- Thurston, C.F., 1994. The structure and function of fungal laccases. *Microbiology* 140, 19–26. <https://doi.org/10.1099/13500872-140-1-19>.
- Tian, Q., Dou, X., Huang, L., Wang, L., Meng, D., Zhai, L., Shen, Y., You, C., Guan, Z., Liao, X., 2020. Characterization of a robust cold-adapted and thermostable laccase from *Pycnoporus* sp. SYBC-L10 with a strong ability for the degradation of tetracycline and oxytetracycline by laccase-mediated oxidation. *J. Hazard. Mater.* 382, 121084. <https://doi.org/10.1016/j.jhazmat.2019.121084>.
- Tsujiyama, S., Muraoka, T., Takada, N., 2013. Biodegradation of 2,4-dichlorophenol by shiitake mushroom (*Lentinula edodes*) using vanillin as an activator. *Biotechnol. Lett.* 35, 1079–1083. <https://doi.org/10.1007/s10529-013-1179-5>.
- Tyanova, S., Temu, T., Sinitcyn, P., Carlson, A., Hein, M.Y., Geiger, T., Mann, M., Cox, J., 2016. The perseus computational platform for comprehensive analysis of (prote) omics data. *Nat. Methods* 13, 731–740. <https://doi.org/10.1038/nmeth.3901>.
- Wang, S., Ning, Y., Wang, S., Zhang, J., Zhang, G., Chen, Q., 2017. Purification, characterization, and cloning of an extracellular laccase with potent dye decolorizing ability from white rot fungus *Cerrena unicolor* GSM-01. *Int. J. Biol. Macromol.* 95, 920–927. <https://doi.org/10.1016/j.ijbiomac.2016.10.079>.
- Wang, M., Yu, H., Wang, P., Chi, Z., Zhang, Z., Dong, B., Dong, H., Yu, K., Yu, H., 2021. Promoted photocatalytic degradation and detoxification performance for norfloxacin on Z-scheme phosphate-doped BiVO<sub>4</sub>/graphene quantum dots/P-doped g-C<sub>3</sub>N<sub>4</sub>. *Sep. Purif. Technol.* 274, 118692. <https://doi.org/10.1016/j.seppur.2021.118692>.
- Wang, S., Zheng, W., Hu, L., Gong, M., Yang, H., 2018. A Powerful and comprehensive web tool for analyzing and visualizing multigroup proteomics data. *J. Comput. Biol.* 25, 1123–1127. <https://doi.org/10.1089/cmb.2018.0050>.
- Weng, S., Ku, K., Lai, H., 2012. The implication of mediators for enhancement of laccase oxidation of sulfonamide antibiotics. *Bioresour. Technol.* 113, 259–264. <https://doi.org/10.1016/j.biortech.2011.12.111>.
- Wiśniewski, J.R., Zougman, A., Nagaraj, N., Mann, M., 2009. Universal sample preparation method for proteome analysis. *Nat. Methods* 6, 359–362. <https://doi.org/10.1038/nmeth.1322>.
- Wong, K., Huang, Q., Au, C., Wang, J., Kwan, H., 2012. Biodegradation of dyes and polyaromatic hydrocarbons by two allelic forms of *Lentinula edodes* laccase expressed from *Pichia pastoris*. *Bioresour. Technol.* 104, 157–164. <https://doi.org/10.1016/j.biortech.2011.10.097>.
- Xu, S., Chen, X., Wang, X., Sun, H., Hou, Z., Cheng, J., Yuan, Y., 2022. Artificial microbial consortium producing oxidases enhanced the biotransformation efficiencies of multi-antibiotics. *J. Hazard. Mater.* 439, 129674. <https://doi.org/10.1016/j.jhazmat.2022.129674>.
- Yadav, R., Rajput, V., Dharne, M.S., 2020. Functional metagenomic landscape of polluted river reveals potential genes involved in degradation of xenobiotic pollutants. *Environ. Res.* 192, 110332. <https://doi.org/10.1016/j.envres.2020.110332>.

- Yan, L., Xu, R., Bian, Y., Li, H., Zhou, Y., 2019. Expression profile of laccase gene family in White-Rot basidiomycete *Lentinula edodes* under different environmental stresses. *Genes* 10, 1045. <https://doi.org/10.3390/genes10121045>.
- Yang, J., Lin, Q., Ng, T., Ye, X., Lin, J., 2014. Purification and characterization of a novel laccase from *Cerrena* sp. HYB07 with dye decolorizing ability. *PLOS One* 9, e110834. <https://doi.org/10.1371/journal.pone.0110834>.
- Yang, X., Lin, R., Xu, K., Guo, L., Yu, H., 2021. Comparative proteomic analysis within the developmental stages of the mushroom white *Hypsizygus marmoreus*. *J. Fungi* 7, 1064. <https://doi.org/10.3390/jof7121064>.
- Yang, J., Lin, Y., Yang, X., Ng, T.B., Ye, X., Lin, J., 2017. Degradation of tetracycline by immobilized laccase and the proposed transformation pathway. *J. Hazard. Mater.* 322, 525–531. <https://doi.org/10.1016/j.jhazmat.2016.10.019>.
- Yu, H., Jiang, N., Yan, M., Cheng, X., Zhang, L., Zhai, D., Liu, J., Zhang, M., Song, C., Yu, H., Li, Q., 2023. Comparative analysis of proteomes and transcriptomes revealed the molecular mechanism of development and nutrition of *Pleurotus giganteus* at different fruiting body development stages. *Front. Nutr.* 10, 1197983 <https://doi.org/10.3389/fnut.2023.1197983>.
- Yu, Y., Yin, H., Peng, H., Lu, G., Dang, Z., 2019b. Proteomic mechanism of decabromodiphenyl ether (BDE-209) biodegradation by *Microbacterium* Y2 and its potential in remediation of BDE-209 contaminated water-sediment system. *J. Hazard. Mater.* 387, 121708 <https://doi.org/10.1016/j.jhazmat.2019.121708>.
- Yu, X., Yin, H., Ye, J., Peng, H., Lu, G., Dang, Z., 2019a. Degradation of Tris-(2-chloroisopropyl) phosphate via UV/TiO<sub>2</sub> photocatalysis: kinetic, pathway, and security risk assessment of degradation intermediates using proteomic analyses. *Chem. Eng. J.* 374, 263–273. <https://doi.org/10.1016/j.cej.2019.05.193>.
- Yu, H., Zhao, S., Guo, L., 2017. Novel gene encoding 5-aminosalicylate 1,2-dioxygenase from *Comamonas* sp. strain QT12 and catalytic properties of the purified enzyme. *J. Bacteriol.* 200 <https://doi.org/10.1128/JB.00395-17>.
- Zhang, S., An, X., Gong, J., Xu, Z., Wang, L., Xia, X., Zhang, Q., 2022. Molecular response of *Anoxybacillus* sp. PDR2 under azo dye stress: an integrated analysis of proteomics and metabolomics. *J. Hazard. Mater.* 438, 129500 <https://doi.org/10.1016/j.jhazmat.2022.129500>.
- Zhang, H., Liu, X., Liu, B., Sun, F., Jing, L., Shao, L., Cui, Y., Yao, Q., Wang, M., Meng, C., Gao, Z., 2023. Synergistic degradation of Azure B and sulfanilamide antibiotics by the white-rot fungus *Trametes versicolor* with an activated ligninolytic enzyme system. *J. Hazard. Mater.* 458, 131939 <https://doi.org/10.1016/j.jhazmat.2023.131939>.
- Zhang, Y.C., Zhou, J., Chen, X., Wang, L., Cai, W., 2019. Coupling of heterogeneous advanced oxidation processes and photocatalysis in efficient degradation of tetracycline hydrochloride by Fe-based MOFs: synergistic effect and degradation pathway. *Chem. Eng. J.* 369, 745–757. <https://doi.org/10.1016/j.cej.2019.03.108>.
- Zhao, S., Chen, X., Sun, Q., Wang, F., Hu, C., Guo, L., Bai, J., Yu, H., 2021. Label-free quantitative proteomic analysis of the global response to indole-3-acetic acid in newly isolated *Pseudomonas* sp. strain LY1. *Front. Microbiol.* 12, 694874 <https://doi.org/10.3389/fmicb.2021.694874>.
- Zhao, S., Pan, C., Zhao, J., Du, H., Li, M., Yu, H., Chen, X., 2022. Quantitative proteomic analysis of the microbial degradation of 3-aminobenzoic acid by *Comamonas* sp. QT12. *Sci. Rep.* 12, 17609 <https://doi.org/10.1038/s41598-022-17570-9>.
- Zougman, A., Selby, P.J., Banks, R.E., 2014. Suspension trapping (STrap) sample preparation method for bottom-up proteomics analysis. *Proteomics* 14. <https://doi.org/10.1002/pmic.201300553> (1006-1000).
- Zuo, Y., Zheng, T., Zhang, Y., Shi, H., Jiang, L., 2022. Facile access to high-efficiency degradation of tetracycline hydrochloride with structural optimization of TiN. *Environ. Sci. Pollut. R.* 29, 36854–36864. <https://doi.org/10.1007/s11356-022-18661-w>.